AL-BALQA APPLIED UNIVERSITY

Hashemite Kingdom of Jordan

Scientific Research Support Fund

Jordanian Journal of Engineering And Chemical Industries

April 2019 | VOLUME 02 | NUMBER 01 | ISSN 2616 - 9584 (Online) ISSN 2616 - 9584 (Print)

JJECI

www.jjeci.com

info@jjeci.com

An International Peer-Reviewed Scientific Journal Financed by the Scientific Research Support Fund

JORDANIAN JOURNAL OF ENGINEERING AND CHEMICAL INDUSTRIES (JJECI)

Jordanian Journal of Engineering and Chemical Industries (JJECI) is an international quarterly peer-reviewed research journal issued by the Scientific Research Fund, Ministry of Higher Education and Scientific Research, Amman, Jordan. JJECI is published by the Deanship of Research, Al-Balqa Applied University, Al-Salt, Jordan. The Journal publishes new and original Research Articles, Short Communications, Technical Notes, Feature Articles and Review Articles encompassing all fields of industrial and chemical engineering fields.

AIMS AND SCOPE

The Journal focuses on broad field of chemical engineering and industrial applications in which original contributions in the following areas appear
Physical Properties and Physical Chemistry
Transport Phenomena and Fluid Engineering
Separation Engineering
Thermal Engineering
Chemical Reaction Engineering
Process Systems Engineering and Safety
Biochemical, Food and Medical Engineering
Nanotechnology
Mathematical Modeling and Computer Simulation
Materials Sciences and Engineering
Energy, Water, Environment and Engineering
Industrial Management and Economics
Oil and Gas Processing
Chemical Engineering Education
Quality control and Standardization
Extractive Metallurgy
Industrial Chemistry

Other related Topics in Chemical Engineering are also welcomed

JJECI ADDRESS

Website: www.jjeci.com
E-mail: info@jjeci.com
Address: Al-Salt, Prince Ghazi Street
P.O.Box: Al-Salt, 19117 Jordan
Telephone: +962-5-3491111
Fax: +962-5-3532312

JORDANIAN JOURNAL OF ENGINEERING AND CHEMICAL INDUSTRIES (JJECI)

TYPES OF CONTRIBUTION

Research Paper: Manuscripts are not to exceed 5000 words excluding references as maximum limit to the length of the research paper including all text, figures, Table and references. It should include a set **of keywords and an abstract followed by Introduction, Materials and Methods, Results and Discussion, Acknowledgments, and References**.

Short Communication: deals with a concise study or preliminary findings that indicate an innovative piece of research that could be less substantial than a full research paper. Short Communication is limited to 2000 words. It should include a set of keywords, an Abstract and a 'Results and Discussion' Section (should be combined) and followed by Conclusion. The number of references is limited to 20 and the number of figures and/or tables is limited to 3.

Letter: Description of novel finding that might not be suitable for a regular research paper or short communication. Letter is limited to 1000 words. The number of references is 10 and the number of figures and/or tables is 2, and 10 references.

Review or mini-review: invited reviews should be of high interest to the readers of the scientific community.

JORDANIAN JOURNAL OF ENGINEERING AND CHEMICAL INDUSTRIES (JJECI)

AIM AND SCOPE:

Jordanian Journal of Engineering and Chemical Industries (JJECI) is an international quarterly peer-reviewed research journal issued by the Scientific Research Fund, Ministry of Higher Education and Scientific Research, Amman, Jordan. JJECI is published by the Deanship of Research, Al-Balqa Applied University, Al-Salt, Jordan. The Journal publishes new and original Research Articles, Short Communications, Technical Notes, Feature Articles and Review Articles encompassing all fields of industrial and chemical engineering fields.

The Journal focuses on broad field of chemical engineering and industrial applications in which original contributions in the following areas appear:

Physical Properties and Physical Chemistry
Transport Phenomena and Fluid Engineering
Separation Engineering
Thermal Engineering
Chemical Reaction Engineering
Process Systems Engineering and Safety
Biochemical, Food and Medical Engineering
Nanotechnology
Mathematical Modeling and Computer Simulation
Materials Sciences and Engineering
Energy, Water , Environment and Engineering
Industrial Management and Economics
Oil and Gas Processing
Chemical Engineering Education
Quality control and Standardization
Extractive Metallurgy
Industrial Chemistry

Other related Topics in Chemical Engineering are also welcomed

JORDANIAN JOURNAL OF ENGINEERING AND CHEMICAL INDUSTRIES (JJECI)

Preparation of Manuscripts

Manuscripts must be written in English typed in one columns fifty-seven lines on numbered pages of A4 or US letter size. All figures and tables should be included in the most appropriate locations within the main text, and not placed on separate pages. A corresponding author will be requested to consent to an agreement transferring copyright on behalf of all authors. All authors will be requested to consent to agreements of submission and authorship.

All authors are encouraged to register or add their ORCID ID when submitting their manuscript or creating their account. The ORCID ID will appear in the published manuscript if an author registers or adds their ORCID ID. Please visit http://www.orcid.org to learn more.

1)Title and authors: This should contain the following items in the given order.

i) Title: The title is to be written in 16 pt. Arial font, centered and using the bold and "Capital Caps" formats. There should be 24 pt. (paragraph) spacing after the last line

ii) Author's names (given name, and surname), affiliations and addresses. If authors' affiliations differ, these should be identified by use of superscripts 1, 2, etc. Identify the corresponding author and give the telephone number, fax number and e-mail address.

iii) If the research has been presented in part at a meeting, give the name, place and date of the meeting.

2) Abstract:

A brief summary (less than 300 words for research papers and journal reviews and 150 words for other types of papers, significant results and conclusions, followed by five keywords. Each keyword should consist of no more than three words.

1) Main Text: main headings will be followed after abstract and keywords by Introduction, Materials and Methods, Results and Discussion, Acknowledgments, and References. Leave a blank line above and below each main heading.
Equations: Number of equations in order with parentheses. Cite as Eq. (1), Eqs. (3) and (5). Spell out "Equation" if at the beginning of a sentence.
Figures and Tables: Each figure and table must have a caption. Cite as Fig. 1, Fig. 2 and 3, and Table 1. Color reproduction will be provided at no cost, if it is essential to clarify the description.

Literature: Cite in the text as follows: Matouq and Tagawa (1960), Matouq and Goto (1989a, 1989b), (Carslaw and Jaeger, 1960), and (Tan and Liou, 1989a, 1989b)
Units: The use of SI units is recommended.
Examples: k[W/(m K)] or k[$Wm^{-1}K^{-1}$], k= 0.58 W/(m K) or k= 0.58 $Wm^{-1}K^{-1}$
Chemical Nomenclature: Use IUPAC or Chemical Abstract conventions.

4) Nomenclature: List symbols in alphabetical order with their definition and SI units. Greek letters, subscripts and superscripts should follow Roman symbols.
5) Literature Cited: Arrange in alphabetical order according to last name of first author, patentee or editor.

1. **Journal Article:** Matouq, M., T. Tagawa and S. Goto, "Micro-channel reactor with guideline structure for organic–aqueous binary system", *J. Chem. Eng. Japan*, **26**, 254–258 (1993)
2. **Book Reference:** Carslaw, H. C. and J. C. Jaeger; Conduction of Heat in Solids, 2nd ed., pp. 198-201, Clarendon Press, Oxford, U.K. (1960).
3. **Chapter in a Book Reference:** Misra NC, Misra S, Chaturvedi A. Carcinoma gallbladder. In: Johnson CD, Taylor I, editors. Recent advances in surgery. London: Churchill Livingstone. 1997; 69-87.
4. **Conference proceedings:** Harnden P, Joffe JK, Jones WG, editors. Germ cell tumours V. Proceedings of the 5th Germ Cell Tumour Conference, 2001 Sep 13-15. Leeds, UK. New York: Springer, 2002.
5. **Dissertation:** Borkowski MM. Infant sleep and feeding: a telephone survey of Hispanic Americans [dissertation]. Mount Pleasant (MI): Central Michigan University. 2002.
6. **Patent:** Primack, H. S.; "Method of Stabilizing Polyvalent Metal Solution," U.S Patent 4, 374,104 (1983),

SUBMISSION OF MANUSCRIPTS

The author must provide a detailed cover letter including a declaration that the work has not been published elsewhere. It is author's sole responsibility that articles publishing from institutions have necessary approvals if needed.

All the articles must be submitted to the email: info@jjeci.com. All the manuscripts submitted should be in the Word (docx, doc format) or PDF format.

Submission of a manuscript implies that it has not previously been published, and is not under consideration for publication elsewhere (except patent disclosure(s) of the author(s)). The Editorial Committee will withdraw a submitted manuscript and retract acceptance and the published article, if any misconduct of publication ethics, which are specified in Guidelines on Publication Ethics for the Journal.

Peer Review Processing:

All articles submitted will undergo double blind peer review processing to meet the international standards. The editor handles the complete editorial process of the articles and peer reviewers remain anonymous to the authors. Editor decisions are strictly followed for quality publications.

AFTER ACCEPTANCE

After acceptance, the author(s) cannot modify the submitted manuscript. Any changes must be addressed through the Editorial office. For the typesetting of the publication, authors will be requested to submit original text and figures online in separate files. All the figures should be of professional quality.

COPYRIGHT

Authors must agree to transferring copyright to the Jordan Journal of Industrial and Chemical Engineering. No article can be published without this agreement.

PROOFS AND REPRINTS

Electronic proofs will be sent as an E-mail attachment to the corresponding author as a PDF file. Page proofs are considered to be the final version of the paper. With the exception of typographical or minor clerical errors, no changes will be made in the paper at the proof stage. Authors will have free electronic access to the full text of the paper. Authors can freely download the PDF file from which they can print unlimited copies of their chapters. Hard copy of

journal issues of which the article appears in will be supplied free of charge to the corresponding author.

PUBLICATION ETHICS

1. **Ethical Standards: JJICE** adheres to the principles of transparency and best ethical practices in scholarly publishing as recommended by the international committees like COPE, DOAJ, OASPA, and WAME.

2. **Plagiarism: JJECI** has strict policies against plagiarism. During the submission, authors require to state that their work is not a copy of another published work and their article is not submitted elsewhere (in full or in part). **JJECI** cross checks every submission for the plagiarism misconduct. Any submission containing partially/completely plagiarized content is rejected immediately.

3. **Attribution Practice:** Citations must be attributed for previously published content. If the authors have used content from any previouslypublished work and fail to provide credit to original source then it will be considered as technical plagiarism and the manuscript might be rejected or retracted.

4. **Conflicts of Interest: JJECI** conduct double blind peer review process to avoid conflicts. The authors should hold responsibility in disclosing any conflicts of interest during article submission to avoid any potential conflicts of interest.

5. **Confidentiality Protection: JJECI** undertakes multiple measures to safeguard the confidentiality and integrity of the authors' work. Editors, peer reviewers and journal staff require maintaining the confidentiality of authors' work. It is ethically not acceptable to use or disseminate the unpublished work.

6. **Human and Animal Rights:** All articles published with **JJECI** must adhere to high ethical standards concerning human volunteers and animal welfare. For animal models and human volunteers ethical clearance letter and documents are required, if applicable.

7. **Consents/Instances:** Authors require obtaining consent for publication from all contributors and participants of the work. Authors must submit the clear statements regarding consents with original signature while submitting their work.

8. **Professional Conduct:** Editors, Reviewers, Authors and the journal staff are expected to adhere to the basic professional courtesy.

Reviewer Guidelines

Peer review is the system for evaluating the quality, validity, and relevance of scholarly research. The process aims to provide authors with constructive feedback from relevant experts which they can use to make improvements to their work, thus ensuring it is of the highest standard possible.

The Review Process

The steps below are the high-level steps in the review process.

Receive Invitation to review

- Accept Invitation
- Review Manuscript
- Submit Review

As a reviewer, you will be notified by e-mail of an invitation to review a manuscript.

- Only agree to review manuscripts for which they have the subject expertise required to carry out a proper assessment and which they can assess in a timely manner.
- Respect the confidentiality of peer review and not reveal any details of a manuscript or its review, during or after the peer-review process, beyond those that are released by the journal.

Double-check the manuscript title page and the Acknowledgments section to determine whether there is any conflict of interest for you (with the authors, their institution, or their funding sources) and whether you can judge the article impartially.

Abstract -Has this been provided (if required)? Does it adequately summarize the key findings/approach of the paper?

Length - Reviewers are asked to consider whether the content of a paper is of sufficient interest to justify its length. Each paper should be of the shortest length required to contain all useful and relevant information, and no longer.

Originality - Is the work relevant and novel? Does it contain significant additional material to that already published?

Presentation –Is the writing style clear and appropriate to the readership? Are any tables or graphics clear to read and labeled appropriately?

References -Does the paper contain the appropriate referencing to provide adequate context for the present work?

Once you've read the paper and have assessed its quality, you need to make a recommendation to the editor regarding publication. The specific decision types used by a journal may vary but the key decisions are:

Accept- if the paper is suitable for publication in its current form.
Minor revision- if the paper will be ready for publication after light revisions. Please list the revisions you would recommend the author makes.
Major revision- if the paper would benefit from substantial changes such as expanded data analysis, widening of the literature review, or rewriting sections of the text.
Reject- if the paper is not suitable for publication with this journal or if the revisions that would need to be undertaken are too fundamental for the submission to continue being considered in its current form.

In your comments intended for the author, do not make statements about the acceptability of a paper (see the next paragraph); suggested revisions should be stated as such and not expressed as conditions of acceptance. Organize your review so that an introductory paragraph summarizes the major findings of the article, gives your overall impression of the paper, and highlights the major shortcomings. This paragraph should be followed by specific, numbered comments, which, if appropriate, may be subdivided into major and minor points. (The numbering facilitates both the editor's letter to the author and evaluation of the author's rebuttal.) Criticism should be presented dispassionately; offensive remarks are not acceptable.

Sometimes you will be asked to review a paper when you do not have sufficient time available. In this situation, you should make the editorial office aware that you are unavailable as soon as possible. It is very helpful if you are able to recommend an alternative expert or someone whose opinion you trust.

If you are unable to complete your report on a paper in the agreed time-frame required by the journal, please inform the editorial office as soon as possible so that the refereeing procedure is not delayed. Make the editors aware of any potential conflicts of interest that may affect the paper under review. Decision of the Editorial Board is final regarding publication of any manuscript.

COPYRIGHT AGREEMENT

JORDANIAN JOURNAL OF ENGINEERING AND CHEMICAL INDUSTRIES (JJECI)

Please complete and sign the form and send it with the final version of your manuscript. It is required to obtain written confirmation from the authors in order to acquire copyrights for papers published in the Journal so as to index them to various repositories.

Title of paper:

_____
_____
_____

Author(s):

_____
_____
_____

The undersigned hereby transfers any and all rights in and to the paper, including, without limitation, all copyrights to the JJECI. The undersigned hereby represents and warrants that the paper is original, is not considered for possible publication elsewhere and that he/she is the author of the paper, except for material that is clearly identified as to its original source, with permission notices from the copyright owners where required. The undersigned represents that he/she has the power and authority to make and execute this assignment.
This agreement is to be signed by corresponding authors and on behalf of co-authors who have obtained the assent of the co-author(s) where applicable.

_____

Author's Signature and Date

_____

Typed or Printed Name

_____

Institution or Company

Jordanian Journal of Engineering and Chemical Industries (JJECI)

Cover Letter/Declaration Form

Date of Submission:

Name of Corresponding Author:

Contact Information of the Corresponding Author

Address:

Email:

Tel:

Article Type:

Manuscript Title:

On behalf of all the co-authors, I am submitting the enclosed manuscript for potential publication only in ***Jordanian Journal of Engineering and Chemical Industries (JJECI).*** I attest that this paper has not been published in whole elsewhere and is prepared following the instructions to authors. All authors have contributed to this manuscript, reviewed and approved the current form of the manuscript to be submitted.

Signature _____
Date_____

Table of contents

Volume 2, Issue 1

The Vapour-Liquid Phase Diagram of Pure Methane Using Temperature Dependent Interaction Parameters: A Monte Carlo Simulation

Ibrahim Suleiman*[1] and Ali Al-Matar[2]

[1]*Al-Balqa Applied University, Faculty of Engineering Technology, Chemical Engineering Department, Amman, Jordan*
[2] *Chemical Engineering Department, Faculty of Engineering and Technology, University of Jordan, Amman, Jordan*

Adopting temperature dependent interaction parameters in the Lennard-Jones potential, the vapour-liquid phase diagram of methane was produced using NVT Gibbs Ensemble Monte Carlo technique. Published second virial coefficient data were used to fit a simple two-parameter temperature dependent model for the interaction parameters. The simulations were carried out in the temperature range 120-190 K. The critical density and temperature were evaluated using Ising-scaling model. Using the temperature dependent interaction parameters in the simulation has reduced the root mean square deviation by 94.7% compared to the temperature independent interaction parameters. The evaluated critical temperature was enhanced using temperature dependent interaction parameters, whereas the simulations using temperature independent interaction parameters predicts a better critical density value.

Keywords: Phase diagram, TDIP, TIIP, Monte Carlo Simulation, Vapor-liquid equilibrium

Introduction

Methane, the major constituent of natural gas, represents a promising alternative energy source. It is also used to calibrate the density transducers which are utilized to directly measure the densities of natural gas transferred in pipelines. It can also be added to some refrigerants to enhance their properties (Betaouaf, *et al*., 2014, Fischer, et al., 1984, Li, *et al*., 2012, Nie, *et al*., 2018, Petropoulou, *et al*., 2018, Ungerer, *et al*., 2007, Uribe-Vargas and Trejo, 2005, Vrabec and Fischer, 1996). Knowledge of thermodynamic properties of methane is necessary to processes of liquefaction, separation, and storage. Therefore, it is required to provide accurate thermodynamic properties of this alkane. Among several models available for modelling the intermolecular forces, Lennard-Jones (LJ) potential have shown to predict accurate results of certain properties of methane (Fischer, *et al*., 1984, Jorgensen, *et al*., 1996, Murad and Gubbins, 1978, Saager and Fischer, 1990, Skarmoutsos, *et al*., 2005, Stassen, 1999); therefore, it has been adopted in this study. Saager and Fischer (SF) (Saager and Fischer, 1990) were able to predict quite accurate simple thermodynamic data of liquid methane using the interaction parameter values 149.9 K and 3.733 Å for the well-depth (ε/k) and collision diameter (σ), respectively. These values were obtained from fitting vapor pressure of methane and liquid densities. Murad and Gubbins (Murad and Gubbins, 1978) have used more complicated five-centered LJ potential to predict more accurate thermodynamic properties of methane. Tchouar *et al.* (Tchouar, *et al*., 2004) have studied the properties of liquid methane at low temperatures and over a large range of pressure using molecular dynamic simulation. They utilized a Feynman-Hibbs temperature dependent potential form which lead to more accurate thermodynamic properties. None of the above-mentioned studies have used temperature dependent interaction parameters (TDIP) model in their simulations. In a previous investigation (Al-Matar, *et al*., 2008, Al-Matar, *et al*., 2015), it has been shown that the usage of TDIP yields to more accurate vapor-liquid equilibrium properties for Argon. In this study, the vapor-liquid equilibrium of methane will be predicted using TDIP and compared with the phase diagram obtained using TIIP, and other modified parameters in the literature.

1 Methodology:

1.1 Intermolecular potential

The Lennard-Jones intermolecular model is used to represent the pair interaction between methane molecules *i* and *j* separated by the distance r_{ij}:

$$u(r_{ij}) = 4\varepsilon_{ij}\left[\left(\frac{\sigma_{ij}}{r_{ij}}\right)^{12} - \left(\frac{\sigma_{ij}}{r_{ij}}\right)^{6}\right] \quad (1)$$

The second virial coefficient *B* was utilized to determine the models of the interaction parameters, ε_{ij} and σ_{ij}, as a function of temperature. An optimization process was carried out aiming to minimize the least squares of the errors between the experimental values of the second virial coefficient (Dymond and Smith, 1980) and those calculated using the equation:

Received on October 18, 2018, accepted on December 9, 2018. Correspondence concerning this article should be addressed to Ibrahim Suleiman (E-mail address: Dr.Ibrahim.Suleiman@bau.edu.jo or Dr.Ibrahim.Suleiman@gmail.com). ORCiD ID of Ibrahim. Suleiman: https://orcid.org/0000-0002-7311-9227

$$B_{classical} = -2\pi N_A \int_0^{\infty} \left[e^{-u(r)/kT} - 1\right] r^2 dr \quad (2)$$

where N_A is the Avogadro's number and k is the Boltzmann constant. This nonlinear optimization problem was solved using Marquardt–Levenberg (Marquardt, 1963, Press, *et al*., 1992) method by minimizing the root mean square deviation (RMSD) value, given by:

$$RMSD = \sqrt{\frac{1}{M}\sum_{i=1}^{M}\left(B_{i,exp} - B_{i,cal}\right)^2} \quad (3)$$

where M is the number of observations, $B_{i,exp}$ and $B_{i,cal}$ are the experimental and calculated second virial coefficient for the *i*th observation, respectively. The integral was evaluated using a 21-point Gauss–Kronrod quadrature to estimate the integral and the associated errors.

Only two-parameter relationships between the independent variable, the temperature, and the dependent variables ε/k and σ, were attempted. These relationships involved combinations of linear, reciprocal, exponential and reciprocal–exponential terms. Only models with parameters that cause σ to increase and ε/k to decrease with temperature were considered feasible (Al-Matar, *et al*., 2008, Al-Matar, *et al*., 2015). The feasible models were subjected to a model discrimination process based on calculating posterior probability (Marquardt, 1963). **Table 1** shows the values of TIIP in the literature and the chosen model of TDIP.

Table 1. Temperature independent values and Temperature dependent models of the interaction parameters.

	ε/k (K)	σ (Å)
Temperature Independent Value (Stassen, 1999)	148.2	3.82
Temperature dependent Model	$144.54 + 2425.014/T$	$4.199 - 55.168/T$

Within the temperature range of interest for methane [120–190 K], used in the simulations which were carried out, the value of σ changes between 3.74 and 3.91 Å, and the value of ε/k changes in the range 164.75 – 157.30 K. While the range of σ is in general agreement with available temperature independent values, the values of ε/k are higher by 6.1-11.2%.

1.2 Simulation Details

Gibbs ensemble is utilized to simulate the coexistence of vapour and liquid phases using systems of 500 atoms. All simulations were carried out with a spherical potential truncation for separations greater than 2.5 σ and tail corrections included. The vapour–liquid simulations were started using two boxes with simple cubic lattice. The number of atoms was equally distributed between the two boxes. The temperature of the entire system is maintained constant and surface effects are avoided by placing each box at the center of a periodic array of identical boxes. The simulations were carried out with 200 equilibration and 2000 production cycles. The type of Monte Carlo moves were selected at random according to the following probabilities: 0.9089 translation, 0.0909 particle swap and 0.0002 volume exchange with one volume exchange per cycle.

The results obtained from the simulations include energy, pressure, density, chemical potential and number of atoms for both vapor and liquid phases. The uncertainties in the ensemble averages were calculated by dividing the post-equilibrium results into ten blocks then taking the grand average (Frenkel and Smit, 1996). The code employed in this work is developed in-house using object oriented programming in FORTRAN-90 and it is available upon request.

1.3 Critical constants

Gibbs ensemble simulations become unstable near the critical region due to the small difference of the free energy between the two phases. According to the scaling law, in the case of Gibbs ensemble simulation, the critical temperature is evaluated by the calculated $\rho - T$ coexistence data (Panagiotopoulos, 1994):

$$\rho_L - \rho_V = b(T_c - T)^{\gamma} \quad (4)$$

Where γ is the non-classical 3D Ising critical exponent ($\gamma = 0.325$). The parameter b and the critical temperature T_c will be obtained from the fit. Subsequently, the critical density ρ_c can be determined using a fit based on the law of rectilinear diameters (Panagiotopoulos, 1994):

$$\frac{(\rho_L + \rho_V)}{2} = \rho_c + A(T_c - T) \quad (5)$$

where the parameter *A* and the critical density ρ_c will be evaluated from the fit.

2. Results and Discussion

The second virial coefficient data was fitted using TIIP as well as TDIP forms. **Figure 1** shows the residuals for the second virial coefficient data of methane using the values available in the literature $\sigma = 3.82$ Å and $\varepsilon/k = 148.2\,K$ (Stassen, 1999), and fitted temperature dependent models, $\sigma = 4.199 - 55.168/T$ and $\varepsilon/k = 144.54 + 2425.014/T$. Using TDIP model yield to closer values of the second virial coefficient than TIIP form. The improvement appears in Figure 1 as the difference between experimental and calculated values decreases in temperature dependent case and gets closer to the zero line than temperature independent case. However, similar to the observation in a previous work (Al-Matar, *et al*., 2008, Al-Matar, *et al*., 2015), the residuals still show systematic trends suggesting that the temperature independent parameters are inadequate to describe the behaviour of the second virial coefficient over a wide temperature range.

Figure 2 compares the simulation results of the vapour–liquid coexistence curve of this work using a TDIP model and the simulation values obtained using TIIP taken from the literature. It also shows the simulation results of Skarmoutsos *et al.*(Skarmoutsos, *et al*., 2005) using Saager-Fischer (Fischer, *et al*., 1984, Saager and Fischer, 1990) model of LJ potential as well as the experimental data (Kleinrahm, *et al*., 1988). A summary of the results using TDIP model is given in **Table 2**.

Table 2. Coexistence energies, pressures and densities, of pure methane for different temperatures at a total number of atoms N = 500

	Energy (J/mol)		Pressure (bar)		Density (g/cm^3)	
Temperature (K)	Liquid	Vapor	Liquid	Vapor	Liquid	Vapor
120	-8331.7	-132.5	9.1	1.34	0.428	2.391×10^{-3}
140	-7398.3	-184.8	1.0	3.15	0.372	4.782×10^{-3}
160	-6506.4	-404.0	1.7	9.30	0.324	1.339×10^{-2}
180	-5612.2	-867.8	21.7	22.0	0.279	3.347×10^{-2}
190	-5205.9	-1797.4	40.93	32.44	0.259	6.873×10^{-2}

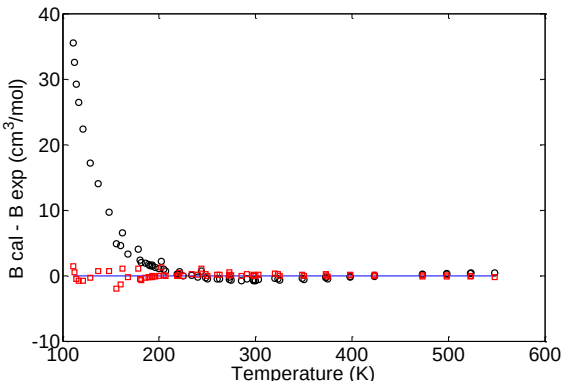

Fig.1. Residuals between experimental second virial coefficient and calculated second virial coefficient. (○ Temperature independent case, □ Temperature dependent case).

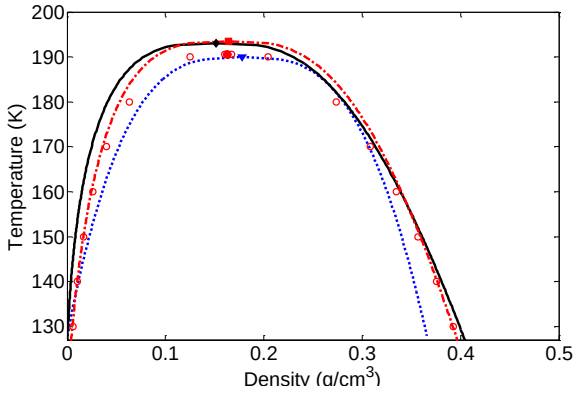

Fig.2. Vapor-liquid phase diagram curve for methane. (○) Experimental data(Kleinrahm, et al., 1988), (.....) temperature independent curve, (-.-.-.-.-)Skarmoutsos - Saager-Fischer model (Skarmoutsos, et al., 2005)–, (——) Temperature dependent curve. ● Experimental critical point, ▼ temperature independent critical point, ■ Skarmoutsos - Saager-Fischer model – critical point, ♦ temperature dependent critical point.

The results of this work obtained using TDIP are closer to the experimental data than the values produced using TIIP. The RMSD values were calculated to be 5.6×10^{-2} and $1.07\ g/cm^3$ for simulations using TDIP and TIIP, respectively (See **Table 3**). The gain in accuracy as measured by the RMSD is, therefore, about 18 folds compared to the TIIP values in the literature. The deviation between the experimental values (Kleinrahm, et al., 1988) of critical density of methane and the predicted results using TDIP and TIIP in the literature are -7.4% and 9.2%, respectively. The vapour-liquid coexistence curve of this work, however, is close to the predicted line by Skarmoutsos *et al.* who adopted the Saager-Fischer (SF) model of LJ potential (Skarmoutsos, et al., 2005). The RMSD obtained using the results of Skarmoutsos *et al.* (Skarmoutsos, et al., 2005) was found to be $4.1 \times 10^{-2}\ g/cm^3$. The RMSD values were calculated from the experimental data (Kleinrahm, *et al*., 1988) of the density in the temperature range [120–190] K.

Saager-Fisher model of *LJ* potential was obtained from fitting vapour pressures and liquid densities; and therefore, it is anticipated that the simulations of Skarmoutsos *et al.*(Skarmoutsos, et al., 2005) produce more accurate values in the liquid region. This procedure has also enhanced the prediction of the critical density (ρ_c). The values of ρ_c are calculated to be $0.151\ g/cm^3$, with 6.9 % deviation from the experimental value, and $0.162\ g/cm^3$, with 0.5 % deviation from the experimental value, using TDIP and TIIP of SF model(Skarmoutsos, *et al*., 2005), respectively. On the other hand the predicted critical temperature using TDIP ($T_c = 193.1\,K$) was more accurate than reported temperature by Skarmoutsos *et al.* ($T_c = 194.3\,K$).

Figure 3 illustrates the vapour pressure versus temperature curves obtained from vapour phase results using TDIP and compares it with the experimental vapour pressure data, as fitted by Antoine equation, for methane. The values of RMSD in vapour pressure of methane using TIIP, TDIP and TIIP-SF model are shown in **Table 4**. The values of RMSD obtained from this work is the highest compared to the results using TIIP and SF model. It is anticipated that using the vapor pressures to fit the LJ potential in the SF model enhances the results of vapor pressure predictions. This is due to fitting the parameters to the vapor pressure of methane. However, compared to a previous investigation (Al-Matar, *et al*., 2008, Al-Matar, *et al*., 2015), the resulting RMSD value in vapour pressure of argon, 6.21 bar, is close to the current RMSD result of methane, 6.57 bar. This indicates that the error in our simulation in vapor pressure has similar trend in both studies.

Table 3. Comparison between critical densities and temperatures for different studies

	$\rho_c\ (kg/m^3)$	$T_c\ (K)$	$RMSD\ (kg/m^3)$
Experimental	162.6	190.6	-
TIIP	178.2	190.0	1.07
TIIP – SF model	161.8	193.5	4.1×10^{-2}
TDIP (this work)	151.4	194.3	5.7×10^{-2}

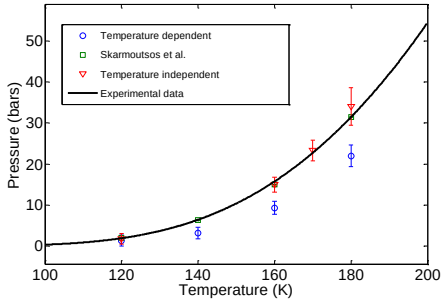

Fig.3. Vapor pressure of methane versus temperature for different systems.

Table 4. RMSD in vapour pressure of methane for cases of TIIP, TIIP-SF model and TDIP

	$RMSD\ (bar)$
TIIP	0.742
TIIP – SF model (Skarmoutsos, et al., 2005)	0.830
TDIP (this work)	6.568

Conclusions

Two parameter models of the interaction parameters, $\sigma = 4.199 - 55.168/T$ and $\varepsilon/k = 144.54 + 2425.014/T$ in LJ potential were used to simulate the vapour-liquid phase diagram of methane. It was shown that using TDIP improves the simulated vapour-liquid coexistence curve of methane modeled as a LJ fluid. Adopting TDIP in the simulations reduces the RMSD of density by 94.7% relative to the values generated using TIIP. However, the predicted critical values were somewhat mixed; as the calculated critical temperature was improved, while the opposite was true for the evaluated critical density. The results of this study are close to the simulations of TIIP using SF model, which has been obtained by fitting the vapour pressure and liquid densities of methane. Their results shows closer values to the experimental data notably in the liquid phase region.

Nomenclature

A	=	Ising scaling law parameter
b	=	Ising scaling law parameter
$B_{classical}$	=	Second virial coefficient in cm^3/mol
$B_{i,cal}$	=	Calculated second virial coefficient
$B_{i,exp}$	=	Experimental second virial coefficient
k	=	Boltzmann Constant
LJ	=	Lennard-Jones
M	=	Number of values
N	=	Number of atoms
N_A	=	Avogadro's Numbers
r	=	Distance in Å
$RMSD$	=	Root mean square deviation
SF	=	Saager-Fischer
T	=	Temperature in K
T_c	=	Critical temperature in K
TDIP	=	Temperature dependent interaction parameters
TIIP	=	Temperature independent interaction parameters
u	=	Interatomic Potential in J
ε_{ij}	=	Well-depth in
γ	=	The non-classical 3D Ising critical exponent $\gamma = 0.325$
ρ_c	=	Critical density in g/cm^3

ρ_L = Density of liquid phase in g/cm^3
ρ_V = Density of vapor phase in g/cm^3
σ_{ij} = Collision Diameter in Å

References

Al-Matar, A.K., Tobgy, A. H. and Suleiman, I.A. "The phase diagram of the Lennard-Jones fluid using temperature dependent interaction parameters". *Molecular Simulation*, **34**, 289-294, (2008).

Al-Matar, A. K., Tobgy, A. H., Suleiman, I. A. and Al-Faiad, M.A. "Improving monte-carlo and molecular dynamics simulation outcomes using temperature-dependent interaction parameters: The case of pure LJ fluid". *International Journal of Computational Methods*, **12 ,** 1550003-1550004-14, (2015)

Betaouaf, F., Cailliez, F., Rousseau, B. and Ould-Kaddour, F. "Molecular simulation of the thermodynamics, structural and transport properties of the liquid binary mixture methane+nitrogen". *Journal of Molecular Liquids*, **200**, 298-304, (2014).

Dymond, J.H. and Smith, E.B. "The Virial Coefficients of Pure Gases and Mixtures" , Second corrected printing, *John Wiley and Sons*, New York, (1980)

Fischer, J., Lustig, R., Breitenfelder-Manske, H. and Lemming, W. "Influence of intermolecular potential parameters on orthobaric properties of fluids consisting of spherical and linear molecules". *Molecular Physics*, **52**, 485-497, (1984).

Frenkel, D. and Smit, B., "Understanding molecular simulation: From algorithms to applications". *Academic Press*, London, (1996).

Jorgensen, W. L., Maxwell, D. S. and Tirado-Rives, J. "Development and testing of the OPLS all-atom force field on conformational energetics and properties of organic liquids". *Journal of the American Chemical Society*, **118**, 11225-11236, (1996).

Kleinrahm, R., Duschek, W., Wagner, W. and Jaeschke, M. "Measurement and correlation of the (pressure, density, temperature) relation of methane in the temperature range from 273.15 K to 323.15 K at pressures up to 8 MPa". *The Journal of Chemical Thermodynamics*, **20**, 621-631, (1988).

Li, Y. F., Yu, Y. X., Zheng, Y.X. and Li, J. D. "Vapor-liquid equilibrium properties for confined binary mixtures involving CO2, CH4, and N-2 from Gibbs ensemble Monte Carlo simulations". *Sci. China-Chem.*, **55**, 1825-1831, (2012).

Marquardt, D. W. "An algorithm for least-squares estimation of nonlinear parameters". *J. Soc. Ind. Appl. Math.*, **11**, 431-441, (1963).

Murad, S. and Gubbins, K. E. "Computer modeling of matter". *ACS Symp. Ser*., **86,** 62-71**,** (1978)

Nie, X., Zhao, L., Deng, S., Su, W. and Zhang, Y. "A review of molecular simulation applied in vapor-liquid equilibria (VLE) estimation of thermodynamic cycles". *Journal of Molecular Liquids*, **264**, 652-674, (2018).

Panagiotopoulos, A. Z. "Molecular simulation of phase coexistence: Finite-size effects and determination of critical parameters for two- and three-dimensional Lennard-Jones fluids". *International Journal of Thermophysics*, **15**, 1057-1072, (1994).

Petropoulou, E., Voutsas, E., Westman, S.F., Austegard, A., Stang, H.G.J. and Løvseth, S.W. "Vapor - liquid equilibrium of the carbon dioxide/methane mixture at three isotherms". *Fluid Phase Equilibria*, **462**, 44-58, (2018).

Press, W. H., Teukolsky, S. A., Vetterling, W. T. and Flannery, B. P. "Numerical Recipes", *Cambridge University Press*, New York, (1992)

Saager, B. and Fischer, J. "Predictive power of effective intermolecular pair potentials: MD simulation results for methane up to 1000 MPa". *Fluid Phase Equilibria*, **57**, 35-46, (1990).

Skarmoutsos, I., Kampanakis, L. I. and Samios, J. "Investigation of the vapor-liquid equilibrium and supercritical phase of pure methane via computer simulations". *Journal of Molecular Liquids*, **117**, 33-41, (2005).

Stassen, H. "On the pair potential in dense fluid methane". *Journal of Molecular Structure: THEOCHEM*, **464**, 107-119, (1999).

Tchouar, N., Ould-Kaddour, F. and Levesque, D. "Computation of the properties of liquid neon, methane, and gas helium at low temperature by the Feynman-Hibbs approach". *Journal of Chemical Physics*, **121**, 7326-7331, (2004).

Ungerer, P., Nieto-Draghi, C., Rousseau, B., Ahunbay, G. and Lachet, V. "Molecular simulation of the thermophysical properties of fluids: From understanding toward quantitative predictions". *Journal of Molecular Liquids*, **134**, 71-89, (2007).

Uribe-Vargas, V. and Trejo, A. "Vapor-liquid equilibrium of methane and methane plus nitrogen and an equimolar hexane plus decane mixture under isothermal conditions". *Fluid Phase Equilibria*, **238**, 95-105, (2005).

Vrabec, J. and Fischer, J. "Vapor-liquid equilibria of binary mixtures containing methane, ethane, and carbon dioxide from molecular simulation". *International Journal of Thermophysics*, **17**, 889-908, (1996).

Optimizing the Performance of Pilot Vacuum Belt Filter (VBF) for P_2O_5 Reduction of Jordanian Phosphogypsum (PG)

Mohammed Aliedeh*

Department of Chemical Engineering, Mutah University, Mutah 61710, Kerak, Jordan

Inventing new ways to recycle and reuse the accumulated byproducts is the most pressing and daunting challenge facing future process engineers. Millions of tonnes of Phosphogypsum (PG) is stacked in Jordan and worldwide every year. Numerous PG laboratory-scale beneficiation methods are already developed. This research is the first in moving PG Beneficiation methods from laboratory scale to pilot-scale using pilot Vacuum Belt Filter (VBF) to clean PG. In this research, VBF Pilot equipment is designed, constructed, troubleshooted and operated. This pilot study affirmed the difficulty in controlling the process input parameters in pilot VBF when compared with batch filtration. Full factorial (2^3) experimental study is conducted to study the effect of number of washings, number of passes, and acid concentration using sulfuric solutions on PG P_2O_5 content reduction. The three studied parameters showed a significant effect and their interaction were significant and contribute significantly to considerable reduction in PG P_2O_5 content. The Pilot VBF were successfully operated to achieve an acceptable reduction of PG P_2O_5 content. In this novel pilot VBF research, numerous process insights were practically gained that significantly helped in optimizing VBF performance in reducing P_2O_5 content in PG.

Keywords: Factorial design; Beneficiation; P_2O_5; Phosphogypsum (PG); Vacuum Belt Filter (VBF); Process Optimization.

Introduction

A huge burden of problems is accumulated in the last century that needs to be tackled. Environmental problems take the lead in these problems that humanity faces nowadays and in the future. Solving these environmental problems by inventing new ways to recycle and reuse the accumulated wastes is one of the major challenges for future process engineers. Jordanian fertilizers industry, which is based on local potash and phosphates resources, is one the major pillars of the Jordanian economy. Jordanian fertilizers industry is mainly based on the production of phosphoric acid. Jordan annual production of phosphoric acid is estimated to be around 500 thousand metric tonnes (Taib, 2011). In addition to this large amount of phosphoric acid, a five times this quantity is stacked every year as Phosphogypsum (PG) in Aqaba, Jordan. Phosphogypsum (PG) is one of the mineral wastes that is accumulated in large a mounts all over the world. The world production of PG is estimated to be 100-280 million tonnes a year that are traditionally stacked in piles. Several impact studies for the stacking of PG show that this practice is uneconomical and adding an ecological burden that in need to be relieved (Reijnders, 2007; Conklin, 1992). Stacks of PG are identified in some 52 countries, including Jordan (Hilton, 2010). PG problem is growing over years and this PG is in need to be utilized (IFA website). PG has been widely tested and piloted for using it for different purposes, such as plasterboard, plaster, cement and soil additive. Moreover, PG can be used for the production of sulfuric acid and manufacture of ammonium sulphate (IFDC/UNIDO Fertilizer manual, 1998). The commercial use of PG in Jordan is currently limited to the production of cement, as agriculture and soil amendment (Al-Hwaiti *et al*., 2010). PG is progressively considered as an asset more than a waste, but its impurities hinders its recycling. PG accommodates small amounts of numerous mineral impurities that phosphate rock contains, or it is produced in the phosphoric acid production process. Phosphorous and Fluor-containing compounds are the most important group of impurities that are present in PG as P_2O_5 and F respectively (Singh, 2003). Therefore, PG cannot be used for other purposes unless these impurities are reduced to the acceptable limits. Reijnders (2007) reported the previously employed methods to reduce the concentrations of minor components in PG. Researchers implemented different methods to clean PG from impurities, such as washing, wet sieving, neutralization with lime, and treatment with a mixture of sulfuric acid and silica or hot aqueous ammonium sulphate solutions (Tayibi, 2009). Many different methods for the reduction of P_2O_5 by chemical and physical methods are already reported in the literature (Saadaouia, *et al*, 2017). Al-Jabbari *et al*. (1988) employed washing PG process with water, sieving it through a 100 μm sieve, and calcining it at different temperatures (low and high). Olmez and Erdem (1989) studied the removal of impurities using several methods based on the neutralization of water-soluble impurities in PG with water and lime milk $Ca(OH)_2$, and a calcining process. Manjit *et al*. (1993) used an aqueous ammonium hydroxide solution (5–20%) to reduce phosphate and fluoride contents in PG. Potgieter *et al*. (2003) studied the effect of chemical and physical treatments of PG used to produce clinker. Klover and Somin (2004) focused their work on the use of a topochemical reaction with an unspecified agent. They claimed that the 226-Ra content of PG can be decreased by a factor of 20–50% and the P_2O_5 content by a factor of 16–28% (Juliastuti, 2018). Aliedeh *et al* (2012 and 2018) studied in batch form the dynamic process of leaching of P_2O_5 in PG. In this study, factorial methodologies is designed to study the effect of particle size, acid concentration, loading and number of washing on the P2O5 washing/leaching process using sulfuric and nitric acid solutions. This Multivariate experimental design analysis helped to understand the relative magnitude of the main and the interaction effects. Sulfuric and nitric acid treatment results shed the light clearly on the role of the number of washing on the reduction of P2O5 content.

Received on January, 22, 2019; accepted on February, 25, 2019 Correspondence concerning this article should be addressed to Mohammed Aliedeh (E-mail address: maliedeh@mutah.edu.jo). ORCiD ID of Mohammed Aliedeh https://orcid.org/0000-0003-4458-7846

The optimum conditions for sulfuric acid treatment is found to be of loading 0.15 g PG/g solution and three washings. The optimum conditions for nitric acid treatment are found to be of a loading 0.4 g PG/g solution and three washings (Aliedeh, 2012, 2018). Al-Hwaiti (2015a) developed different treatments methods for phosphogypsum: (1) hybrid water, (2) sulphuric acid, (3) mixed acid (H2SO4 and HNO3), (4) household water (tap water and distilled water) and (5) calcium carbonate powder treatment. These treatments are designed to remove and leach the activity concentrations of ^{226}Ra, ^{232}Th, and ^{40}K in the samples of Jordanian phosphogypsum. Al-Hwaiti (2015b) has utilized an inexpensive adsorbent system for the removal of heavy metals from PG using polyethylene glycol and polyvinyl alcohol. This study investigated the performance these two polymers (PEG and PVA) in removing heavy metal from PG with a batch reaction approach. The above literature review shows that most of the reported research is focusing on lab scale batch experimental processes without stepping further to pilot scale. Kovler *et al*. (2015) stressed that known PG purification approaches have failed to produce a breakthrough in the industry, and is still confined to the laboratory, largely due to efficiency and cost considerations. Kovler *et al*. (2015) called for a cooperation between academic and industrial partners in order to move laboratory-scale approaches to a larger pilot-scale. Aliedeh *et al* (2012 and 2018) studied in a batch setup the dynamic process of P_2O_5 reduction in PG through developing pilot plant model which paved the road to move the PG beneficiation process from Laboratory-Scale to pilot-scale. This research aims to develop and optimize the performance of a pilot scale VBF process for PG beneficiation and to investigate P_2O_5 reduction using an optimized Pilot Vacuum Belt Filter (VBF) Process.

1 Design Methodology: Developing Pilot-Scale VBF

1.1 Wet-Process of Phosphoric Acid Production

There are two basic types of processes for the production of phosphoric acid; furnace processes and wet processes. Commercial wet processes may be classified according to the hydrate form in which the calcium sulfate crystallizes: Anhydrite -$CaSO_4$, Hemihydrate – $CaSO_4.1/2\ H_2O$, and Dihydrate- $CaSO_4.2H_2O$ (Singh, 2003). As simple dehydrate process flow sheet is shown in **Figure 1** (Singh, 2003). The role of the filtration and washing process in the wet process aims to separate the produced gypsum from any insoluble materials derived from phosphate rock or formed in the reaction from the phosphoric acid product. All modern plants use only horizontal vacuum belt filters (VBF) (IFDC/UNIDO Fertilizer manual, 1998). The only type of filters that are suitable for phosphoric acid production (Fig. 1) are the horizontal vacuum belt filters (VBFs), which are offered by companies such as Fimco, Delkor, and Pannevis (IFDC/UNIDO Fertilizer manual, 1998).

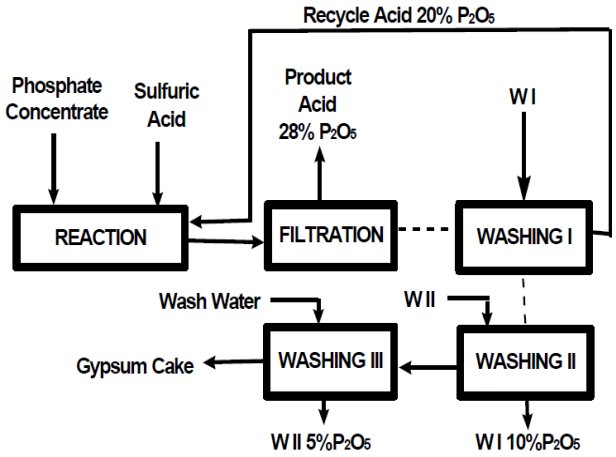

Fig. 1. Simple Dihydrate Process Flow sheet (Singh, 2003)

1.2 Successful Applications of Vacuum Belt Filters

Vacuum belt filters (VBFs) can be applied to many different slurries, including fibrous materials, fine slimes, and coarse granular solids. They provide high extraction efficiency, low cake moisture, increased production and reduced operating costs. VBFs are especially suited for applications requiring low cake moisture and multi-stage washing. Low energy consumption and high filtration rate make VBFs an excellent choice for a wide range of industrial processes (Smidth, 2010). Therefore, VBF is chosen as the equipment to move the PG beneficiation research from the laboratory-scale to the pilot-scale. Moreover, It is implemented in the PG beneficiation research in order to be smoothly integrated in the existing industrial wet phosphoric acid production processes. Horizontal Vacuum Belt Filters are already implemented in almost all wet phosphoric acid plants to separate and wash PG from phosphoric acid solution and its impurities. VBF is characterized by being easily manipulated through controlling slurry feed rate, cake thickness, belt speed, vacuum level, recycling between stages, number of stages, washing rate, racking type, …etc. Aliedeh *et al*. 2012 and 2018 did a screen analysis for Jordanian PG and it is found that the PG has a wide spectrum of sizes and it is not, as mentioned, extremely fine. Racking is used in this research to overcome cake resistance. The dynamic manipulation of input parameters in VBF is encouraging implementing it as a tool for PG Abatement.

Fig. 2. Main components of the designed Pilot VBF**.**

1.3 Designing the Pilot VBF

Based on the established VBF operating guidelines (Smidth, 2010), the Pilot *VBF Process* is designed of three stages: cake formation, cake washing and cake dewatering, as illustrated in **Fig. 2.** The three stages are assembled together to create a one pass of rotating belt filter. Each stage is equipped with a separate filtrate collecting tank that is fitted under the top plate to enable the creation of vacuum in these three trays through connecting them with three separate vacuum pumps, as illustrated in
. The first stage is equipped with a mixing tank
and slurry feed distributer for the PG slurry feed to the cloth and the third stage is equipped with dry cake scrapping mechanism and a collection container. The dimensions of these numerous Pilot RBF components are shown in **Fig. 4.**

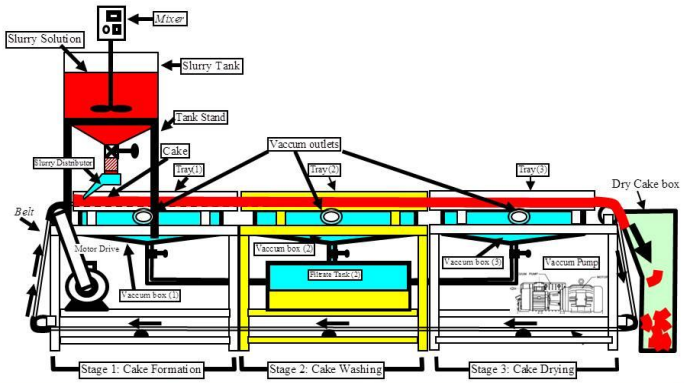

Fig. 3. Pictures of the designed pilot VBF.

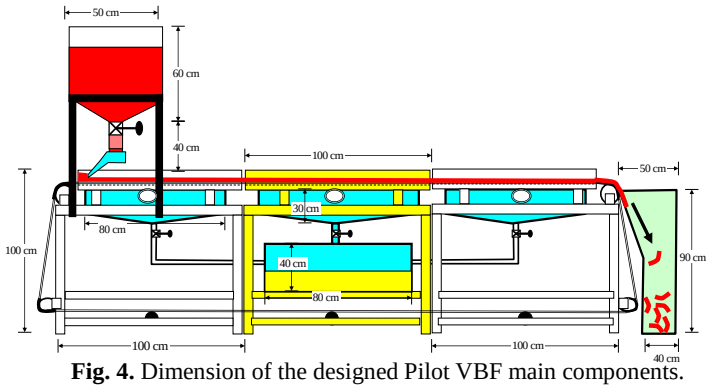

Fig. 4. Dimension of the designed Pilot VBF main components.

1.4 Building and Troubleshooting of Pilot VBF

The construction, troubleshooting and operation of this Pilot RBF was a long and daunting process that includes solving the numerous operational challenges and problems such as: slipping of the cloth off the drums and switching to Chaining the rotating cloth; the failure of vacuum build-up and the enhancement of the dewatering process; slurry distributor Problem due to PG solidification; devising an effective mechanism for controlling cake thickness; The selection of an appropriate locally available filter cloth; and proper connection of cloth ends. Even with all these challenges, the researcher achieved the main goal of moving the PG beneficiation process from the laboratory scale to the pilot VBF pilot scale.

2 Experimental Methodology: Running Pilot-Scale VBF

2.1 Raw Materials

PG samples were collected from Arab Phosphate Co. /Industrial Complex, Aqaba, Jordan. The samples were produced by the dihydrate process. This sample was analyzed for chemical constituents and compared with the composition of PG from other sources as listed in **Table 1**.

Table 1. Chemical compositions of Jordanian PG in comparison to other sources (Aliedeh, *et al*, 2012, 2018)

Chemical Compound	PG1*	PG2**	PG3**	PG4**
H_2O	20	19.5	20.0	18.0
SO_2	47.6	43.2	44.0	43.6
CaO	32.60	32.2	31.0	32.0
MgO	0.01	0.01	--	0.40
$Al_2O_3 + Fe_2O_3$	0.173	0.27	0.14	1.82
SiO_2	1.46	1.51	2.40	1.64
Na_2O	0.15	0.47	0.18	0.36
P_2O_5 (total)	1.07	1.01	0.78	1.03
F (total)	0.61	1.67	0.57	0.76
Organic Matter	0.14	0.08	0.24	0.26

* In this study PG1= Arab Phosphate Co., Industrial complex, Aqaba Jordan
** Chandra, S., 1997, PG2= morocco, PG3= Florida, USA, PG4= India
Chemicals: (1) Reagent grade H_2SO_4 , (2) Local tap water.)

2.2 Determination of Phosphates by the Gravimetric Quimociac Technique

Gravimetric Quimociac Technique is based on first converting all the phosphorus-containing species in the sample to soluble orthophosphate (PO_4^{3-}) ion by oxidation and hydrolysis in acid solution. When an acidic quimociac reagent is added to the prepared orthophosphate sample and a bright yellow precipitate forms. The resulting precipitate is filtered, dried and weighed. Precipitation is described by the following reaction (Shaver, 2008):

$$H_3PO_4+12H_2MoO_4+3(C_9H_7N)\rightarrow(C_9H_7N)_2\cdot H_3PO_4\cdot 12MoO_3\cdot H_2O+11H_2O$$

{Yellow precipitate } (1)

When the precipitate is dried, the water of hydration is removed, leaving a stable, anhydrous, yellow product with a molar mass of 2213 g/mol.

***Preparation of the Quimociac solution*:**

1. Dissolve 70g of Sodium molybdate dehydrate ($Na_2MoO_4.2H_2O$) in 150ml distilled water.

2. Dissolve 60g of Citric Acid Monohdrate ($C_6H_8O_7.H_2O$) in 150ml distilled water, and then add 85ml nitric acid (HNO_3).
3. Gradually add the molybdate solution to the citric-nitric acid solution while stirring.
4. Dissolve 5mL synthetic quinoline, with stirring, in a mixture of 35mL of concentrated HNO_3 and 100mL H_2O.
5. Gradually add this solution to the molybdic-nitric acid solution, mix well and let stand for 24 hours.
6. Filter, add 280mL of acetone, dilute to 1L with H_2O, and mix.
7. Store in either a noncolored polyethylene bottle or a dark brown glass bottle.

***Method of Examination*:**

1. Arrange samples and place them inside porcelain crucibles.
2. Place the samples in a thermal oven at 105°C, and leave them for 2 hours.
3. Weight 2.00g of the sample by an analytical balance (±0.0001 accuracy)
4. Put it in a conical flask.
5. Add 25ml of digestion solution consisting of:
   20% HCl.
   40% HNO_3.
   40% H_2O.
6. Put the sample into electrical heater, until the sample becomes colorless.
7. Add 50ml of distilled water.
8. Leave samples for five minutes to get to room temperature.
9. Put the solution in volumetric flask, and then add distilled water to the solution until fully filled (250 ml).
10. Recap volumetric flask tightly and then shake the solution very well.
11. Filter the solution by filter paper.
12. Draw 50 ml (aliquot) of filtered sample by pipette, and place in a beaker.
13. Add 25 ml of nitric acid solution consisting of:
    33.33% HNO_3.
    66.66% H_2O.
14. Add 25ml of Quimociac solution.
15. Place the solution on an electric heater until it becomes a dark yellow color.
16. Leave samples for five minutes to get to room temperature.
17. Weight the crucibles.
18. Filter sample by vacuum pump filter.
19. Put the crucibles in a thermal oven at 105°C, and leave for 2.5 hours.
20. Calculate the wt of the precipitate
21. Calculate $\%P_2O_5$ based on the following equation:

$$\text{Percent } P_2O_5 = \frac{\overbrace{\overbrace{\dfrac{(\text{g precipitate})}{\left(2213\dfrac{\text{g precipitate}}{\text{mol precipitate}}\right)}}^{\text{mol precipitate}}\left(\dfrac{\text{mol } P_2O_5}{2\text{ mol precipitate}}\right)\left(141.9\dfrac{\text{g } P_2O_5}{\text{mol } P_2O_5}\right)\left(\begin{matrix}\text{Sample}\\ \text{Volme Ratio}\end{matrix}\right)}^{\text{g } P_2O_5 \text{ in sample aliquot}}}{(\text{g sample})}(100\%) \quad \overbrace{\qquad\qquad}^{\text{g } P_2O_5 \text{ in sample solution}}$$

(2)

Which can be arranged to result in:

$$\text{Percent } P_2O_5 = \frac{(\text{g precipitate})\left(141.9\dfrac{\text{g } P_2O_5}{\text{mol } P_2O_5}\right)\left(\begin{matrix}\text{Sample}\\ \text{Volme Ratio}\end{matrix}\right)(100\%)}{\left(2213\dfrac{\text{g precipitate}}{\text{mol precipitate}}\right)\left(2\dfrac{\text{mol precipitate}}{\text{mol } P_2O_5}\right)(\text{g sample})} \tag{3}$$

$$\left(\begin{matrix}\text{Sample}\\ \text{Volme Ratio}\end{matrix}\right) = \frac{\text{volume sample solution}}{\text{volume sample aliquot}} = \frac{250\text{ ml}}{50\text{ ml}} \tag{4}$$

2.3 Factorial Design Methodology

Experimental designs are plans for determining how one or more experiments are to be run. Experimental strategies range from trial-and-error testing through one- factor or variable-at-a-time testing (OVAAT) to what is more commonly considered Design of Experiments (DOE) such as factorial designs (Smidth, 2010; Moalla, 2018). Full factorial design (23) is implemented in this research because it allows measurement of the main effects in addition to the interaction effects needed to obtain high levels of complex process understanding. The Full factorial design of 23 is implemented with three input parameters that are selected to be studied: (1) Number of washing, (2) number of Passes, and the concentration of aqueous solution, as listed in two replicates for each run is accomplished in addition to six center points as shown in the design matrix listed in Error! Reference source not found.**3**.

Table 2. The selected values of input parameters in the full factorial experimental design matrix

Input Parameters	Low	Center	High
# of Washing (A)	1	2	3
# of passes (B)	1	2	3
% H_2SO_4 (w/w) (C)	1	3	5

2.4 VBF Pilot Plant Operating Conditions

The PG samples where thoroughly mixed with aqueous sulphuric Acid solution in the feed tank for 30 minutes. The PG/ Sulfuric Acid Solution mixture is processed through the VBF pilot equipment based on the operating conditions listed in **4**. The control of these important process parameters was an added challenge to the experimental work accomplished. Some variation is noticed in some of these experimental operating conditions such as washing rate, film thickness, Solution ration due to settling and feed rate. These sources of variability are widening the range of variation in the P_2O_5 reduction achieved.

3 Results and Discussion

Full ANOVA analysis is applied to the 2^3 full factorial design of pilot study (The Design matrix is shown in **Figure 1**) using Minitab® 16 software, as listed in Error! Reference source not found.. The ANOVA analysis results are plotted in the form of Pareto chart (Fog 1) to show the significance of each studied input variable effects.

3.1 Main effects

The significance of input variables are determined based on the value of probability p. Full ANOVA analysis shows that the number of washes (A), the number of passes (B) and Acid Concentration (C) were significant within the 95% confidence interval ($p \leq 0.05$). These three input variables are expected to play an important role in reducing the PG P_2O_5 content. These results agrees well with the previous published batch dynamic results (Aliedeh, 2012 and 2018), i.e. the more number of washes, number of passes and higher acid concentration significantly contribute to more reduction in PG P_2O_5 content (Error! Reference source not found. and Error! Reference source not found.). This indicates that the pilot VBF is functioning properly and it can be a good basis to move towards pilot plant scale.

Table 3. VBF pilot equipment based on the operating conditions

Operating Conditions	Condition Value
PG/ Solution Ratio	0.5 g PG / g Solution
PG mixture feed rate to VBF	0.25 kg PG mixture/minute
Film thickness	3-5 mm
Washing rate	0.5 liter/minute
Filtration Belt Moving Speed	1.5 m/ minute
Cloth Material	Polyester (PET)

3.2 Interaction effects

This study is based on the multivariate experimental work; therefore, interaction effects must be discussed with the main effects. Factorial design methodology has the ability to reveal the interaction between the input parameters under study. The focus in this study will be on the two-factor interactions. **Fig. 7** shows the two factor interaction plots for the study of VBF P_2O_5 reduction by sulphuric acid solution. These plots show that all the interactions are almost significant. Strong interaction is observed between: the number of passes (B) and the acid solution concentration (C), the number of washes (A) and the acid solution concentration (C), but a weak interaction is clear between the number of washes (A) and number of passes (B)

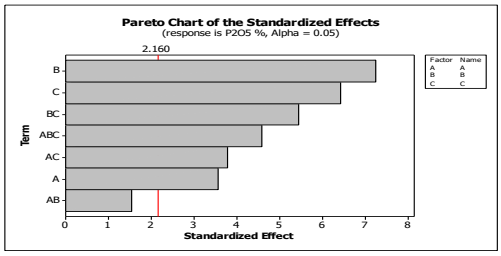

Fig. 5. Puerto chart for sulfuric acid treatment 2^3 full factorial design experiments.

Table 4. Experimental design matrix and results for P_2O_5 wt% in Pilot VBF treated PG samples using Sulfuric Acid Solution

Term	Effect	Coef	SE Coef	T	P
Constant		0.6526	0.01017	64.16	0
A	-0.0726	-0.0363	0.01017	-3.57	0.003
B	-0.1475	-0.0737	0.01017	-7.25	0
C	-0.1305	-0.0653	0.01017	-6.42	0
A*B	0.0313	0.0156	0.01017	1.54	0.148
A*C	-0.0771	-0.0385	0.01017	-3.79	0.002
B*C	-0.1106	-0.0553	0.01017	-5.44	0
A*B*C	-0.0933	-0.0467	0.01017	-4.59	0.001
Ct Pt		-0.1123	0.01948	-5.76	0

Coef= Regression Coefficient , SE Coef= Standard Error of Regression Coefficient, T= Student's t Distribution Value, P= Probability Value for t Distribution

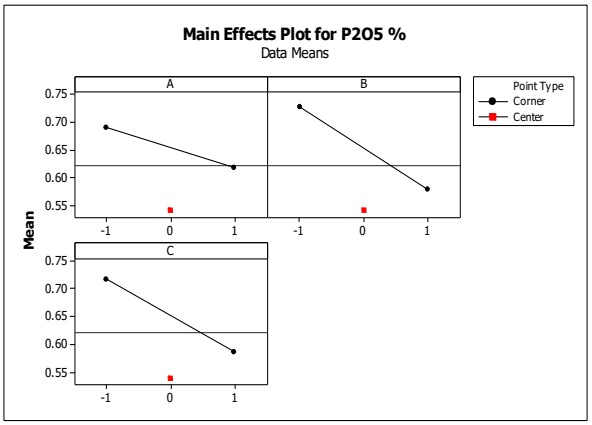

Fig. 6. Main effect plots for sulfuric acid treatment 2^3 full factorial design experiment

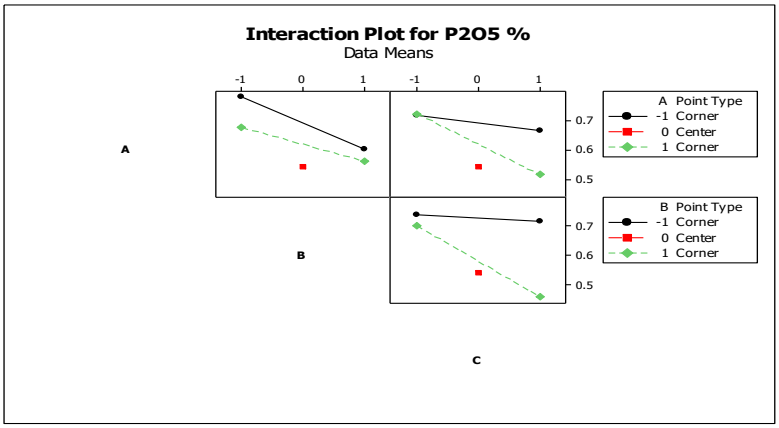

Fig. 7. Interaction effects for sulfuric acid treatment 2^4 full factorial design experiment

This interaction behavior totally agrees with the interaction pattern that was reported in Aliedeh *et al*. (2012 and 2018) batch dynamic studies. These strong interaction effects can contribute to affect a change in P_2O_5 reduction behavior. The results show the selection of input parameters in both batch dynamic studies (Aliedeh, 2012 and 2018) and the pilot VBF study was successful and both agrees on the most important parameters that the P_2O_5 reduction process should focus on (number of washing, number of passes, and acid concentration). These three important process parameters and their interactions is integrated to get a considerable reduction in P_2O_5 content. Based on the above discussion of the results, it should be noted that the sources of errors and interference in pilot scale experiments are significantly more pronounced than in batch wise experiments. The control of errors in continuous pilot plant studies is very difficult and requires long experience in running these pilot plants effectively. Despite these challenges, both the previous batch dynamic studies and this pilot VBF research successfully achieved an acceptable amount of P_2O_5 content reduction and clearly identified the most important input parameters that strongly contribute to the PG P_2O_5 content reduction process.

Table 5. Full 2^3 factorial design for P_2O_5 wt% in VBF treated PG samples using Sulfuric Acid solution

Run	No. of Washes	No. of Passes	% H_2SO_4	No. of Washes	No. of Passes	% H_2SO_4	% P2O5
1	-1	-1	-1	1	1	1	0.7648
2	+1	-1	-1	3	1	1	0.6642
3	-1	+1	-1	1	3	1	0.5708
4	+1	+1	-1	3	3	1	0.736
5	-1	-1	+1	1	1	5	0.7551
6	+1	-1	+1	3	1	5	0.6231
7	-1	+1	+1	1	3	5	0.5432
8	+1	+1	+1	3	3	5	0.3384
9	-1	-1	-1	1	1	1	0.828
10	+1	-1	-1	3	1	1	0.6883
11	-1	+1	-1	1	3	1	0.6991
12	+1	+1	-1	3	3	1	0.792
13	-1	-1	+1	1	1	5	0.7654
14	+1	-1	+1	3	1	5	0.7221
15	-1	+1	+1	1	3	5	0.5852
16	+1	+1	+1	3	3	5	0.3665
17	0	0	0	2	2	3	0.5048
18	0	0	0	2	2	3	0.5576
19	0	0	0	2	2	3	0.5288
20	0	0	0	2	2	3	0.5767
21	0	0	0	2	2	3	0.5279
22	0	0	0	2	2	3	0.5463

The strong effect of the number of washings stressed the importance of maintain an effective washing process by: (1) controlling effectively the PG slurry thickness (2) minimizing channeling during cake washing over the filter cloth by slice fragmentation, as illustrated in Fig. 8. These cake washing problems did not show up in dynamic batch results experiment (Aliedeh, *et al*. 2012 and 2018),because a buchner funnel filtration was used in which a film thickness of 2-3 mm and a highly controlled washing is affected by spraying water all over the buchner funnel and manually ploughing the PG cake formed, see Fig. 9. It is recommended that more attention should be given to a new pattern of ploughing the cake in order to enhance its washing process over the rotating filter cloth, as illustrated in Fig. 9. Further current research in our labs is being accomplished to handle the above mentioned problems.

Fig. 8. Photographs of racking patterns of the PG cake while moving over the rotation belt

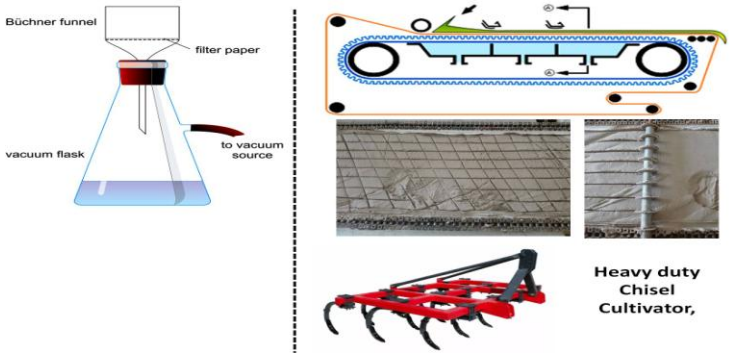

Fig. 9. The need to plough the filtered cake to enhance the washing over the belt

Acknowledgments

This work was supported by The Jordanian Scientific Research Support Fund (SRRF) [Grant number: Eng/2/12/2013]. The author acknowledges Eng. Atif Altarawneh for laboratory support.

Nomenclature

g precipitate	=	mass of precipitate	[g]
Percent P_2O_5	=	mass percent of P_2O_5	[m]
g samle	=	mass of PG solid samples used for analysis	[g]

References

Al-Hwaiti, M "Assessment of the radiological impacts of utilizing treatment phosphogypsum as main constituent in the building materials in Jordan" *Env. Earth Sci.*, ***74,*** 3159-3169, (2015)

Al-Hwaiti, M., Araf, K, Harara, M. "Removal of heavy metals from waste phosphogypsum materials using polyethylene glycol and polyvinyl alcohol methods". *Arabian Journal of chemistry*. (2015b).

Al-Hwaiti, M., Ross, P., Ranville, J. "Bioavailability and mobility of trace metals in phosphogypsum from Aqaba and Eshidiya, Jordan" *The Chemie der Erde Geochemistry*, **70**, 283-291, (2010b).

Aliedeh, M. A. "The implementation of factorial experimental design to optimize phosphogypsum beneficiation process (P2O5 reduction) using sulfuric and nitric acids solutions" *Jour. of Chem. Tech. and Metallurgy*, **53**, 437-450, (2018).

Aliedeh, M. A., and Jarrah, N. A. "Application of full factorial design to optimize phosphogypsum beneficiation process (P2O5 reduction) by using sulfuric and nitric acid solutions", *Sixth Jordanian International Chemical Engineering Conference*, , Amman, Jordan (2012).

Al-Jabbari, S., Faisal, F., Ali, S., Nasir, S. "Environmental impact and management of phosphogypsum" , *Journal of Building Research, Scientific Research Council*, Baghdad **7**, 49, (1988).

Chandra, S. "Waste materials used in concrete manufacturing", Noyes Publications (1997).

Conklin, C. "Potential uses of phosphogypsum and associated risks", US Environmental Protection Agency (1992).

Fertilizer manual: this manual is a successor to and in part a revision of the IFDC/UNIDO Fertilizer manual published in December 1979. Kluwer academic Publishers, (1998).

Smidth F. "EIMCO Extractor Horizontal Belt Filter" *Minerals Processing Technology Center*, F L Smidth Salt Lake City, Inc, (2010).

Hilton, J. "Phosphogypsum (PG):uses and current handling practices worldwide" *25th Annual Lakeland Regional Phosphate Conference* (2010).

International Fertilizer Association (IFA), "Sustainable development and the fertilizer industry Phosphogypsum: From waste to co-product" http://www.fertilizer.org/ifa/HomePage/SUSTAINABILITY/Sustainable-development/Phosphogypsum.html

Juliastuti, S. R., Hendrianie, N., Pawitra1,Y. D. and Putra, I. R "Reduction of P_2O_5 and F from phosphogypsum by CaO addition" *MATEC* Web of Conferences **156**, 138-140, (2018).

Kovler, K., Dashevsky, B., Kosson, S."Purification of phosphogypsum from ^{226}Ra and heavy metals for its further utilization in construction: technological utopia or reality", Research Poster, Conference "*Exchange Of Good Practices On Metal By-Products*, 12-13, (2015)

Kovler, K., Somin, M. "Producing environment-conscious building materials from contaminated phosphogypsum" Technion, Haifa, (2004).

Manjit, S., Garg, M., Rehsi, S.S: "Purifying phosphogypsum for cement manufacture" *Construction and Building Materials* **7**, 3-7, (1993)

Moalla, R., Gargouri, M., Khmiri, F., Kamoun, L., Zairi, M. "Phosphogypsum purification for plaster production: A process optimization using full factorial design" *Envi.. Eng. Res.*, **23**, 36-45, (2018).

Olmez, H., Erdem, E. "The effect of phosphogypsum on the setting and mechanical properties of Portland cement and trass cement", *Cement and Concrete Research* **19**, 337–384, (1989)

Potgieter, J. H., Potgieter, S. S., McCrindle, R. I., Strydom, C. A. "An investigation into the effect of various chemical and physical treatments of a South African phosphogypsum to render it suitable as a set retarder for cement" *Cement and Concrete Research*, **33**, 1223–1227, (2003).

Reijnders, L. "Cleaner phosphogypsum, coal combustion ashes and waste incineration ashes for application in building materials: A review" *Building and Environment* **42**, 1036–1042, (2007).

Saadaouia, E., N. Ghazela, C. B. Romdhanea and N. Massoudic, “Phosphogypsum: potential uses and problems – a review” International *Jour. of Envi. Studies*, **74**, 558–567, (2017)
Shaver, L. "Determination of Phosphates by the Gravimetric Quimociac Technique" *Jour. of Chem. Edu.*, **85**, 1097-1098, (2008).
Singh, M.: “Effect of phosphatic and fluoride impurities of phosphogypsum on the properties of selenite plaster” *Cement and Concrete Research*, **33**, 1363–1369, (2003)
Taib, M., “The mineral industry of Jordan”, 2009 Minerals Yearbook- Jordan Advance Release, USGS (February 2011).
Tayibi, H., Choura, M., López, F. A., Alguacil, F. J., & López-Delgado, A. "Environmental impact and management of phosphogypsum", *Jour. of Env. Manag.*, **90**, 2377-2386, (2009)

Identifying the Effect of Non-Ideal Mixing on a Pre-Denitrification Activated Sludge System Performance through Model Based Simulations

Malek Hajaya[1]

[1]*Civil Engineering Department, Tafila Technical University, Tafila 66110, Jordan*

Effectiveness of a pre-denitrification activated sludge treatment system is governed by the kinetics of the biological reactions, and the hydrodynamic mixing behavior in the reactors. Achieving good mixing conditions within a reactor not only enhances the transfer of reactants, but also insures homogeneous environmental conditions throughout the vessel when required, allowing for an effective usage of the reactor's total volume, leading to optimized, low cost operation. In this work, a pre-denitrification activated sludge system performance with regards to the biological treatment of organic carbon and nitrogen was investigated, under two scenarios for non-ideal mixing in the anoxic reactor. The system performance is simulated based upon the Activated Sludge Model 1 model's biological reactions, and combining two non-ideal mixing two parameter models: CSTR with bypass and dead volume, and two CSTRs with exchange. Performance discrepancies were then identified in the presence of non-ideal mixing. The system's performance was found to be more susceptible to the presence of a dead volume/bypass scenario compared to the two CSTRs with material exchange scenario. Under non-ideal mixing conditions, effluent concentrations of Total Kjeldahl Nitrogen, organic carbon increased marginally, while effluent concentration of nitrate increased significantly. Similarly, the waste stream concentrations of Total Kjeldahl Nitrogen and organic carbon increased significantly as a result to an increase in the concentration of the heterotrophic biomass. The outcome of this study provides an insight when trouble shooting the operation of pre-denitrification activated sludge systems for non-ideal mixing conditions.

Keywords: Non-ideal mixing, Activated sludge, Dead volume, Bypass, Material exchange

Introduction

Activated Sludge (AS) systems are among the most widely employed biological treatment processes in wastewater treatment plants(Rittmann and McCarty, 2001). AS systems are engineered processes, designed and operated to sustain and facilitate the growth of different microorganisms. These microorganisms in their part treat wastewaters biologically by incorporating/removing the pollutants in their different metabolic and growth associated processes. Those pollutants are mainly comprised from dissolved and particulate organic carbon and nitrogen containing compounds. The main biological processes leading to wastewater treatment taking place in AS systems, and the associated microorganisms responsible for them are: organic carbon mineralization under aerobic and anoxic conditions by facultative heterotrophic bacteria, ammonia (NH_3) oxidization under aerobic conditions to nitrate (NO_3^{-1}) by autotrophic nitrifying bacteria, and nitrate reduction under anoxic conditions to nitrogen gas (N_2) by the aforementioned facultative heterotrophic bacteria (utilized instead of oxygen in the metabolic process) (Madigan and Martinko, 2006; Tchobanoglous *et al*., 2007). Pre-denitrification is (PD) one approach for the operation of AS (Hellinga *et al*., 1999; Kim *et al*., 2009). The required environmental conditions (anoxic and aerobic) are divided between two distinctive Continuous-flow stirred-tank reactors (CSTRs), and the microorganisms (biomass) are circulated between them. **Figure 1** illustrates the process scheme. The anoxic reactor receives both fresh organic carbon and ammonia containing wastewater and a nitrate-rich, biomass containing, mixed liquor recycle from the aerobic reactor, where a portion of organic carbon is mineralized and nitrate is reduced to nitrogen gas. Anoxic reactor effluent carries the remaining untreated wastewater to the aerobic reactor, where air is supplied to sustain an elevated oxygen concentration, and enhanced mixing conditions. The remaining organic carbon is completely mineralized and ammonia is oxidized to nitrate. The settler allows for biomass to be separated from the mixed liquor, and recycled back so that the system's solids retention time is controlled independently from the system's hydraulic retention time (Tchobanoglous *et al*., 2007). Effectiveness of a PD-AS treatment system is governed by the kinetics of the biological reactions, and the hydrodynamics of mixing in the reactors. The different reactions and processes taking place in a PD-AS system were first identified and modeled by the International Water Association (IWA) Activated Sludge Model 1 (ASM1) (Henze *et al*., 2000), and since employed in a wide variety of studies (Alex *et al*., 2008; Hajaya and Pavlostathis, 2013; Ostace *et al*., 2011; Van Loosdrecht *et al*., 2015). ideal mixing conditions are commonly assumed while designing biological reactors for wastewater treatment processes (Vanrolleghem *et al*., 2003). Achieving good mixing conditions within reactors not only enhances the transfer of substrates (reactants), but also insures homogeneous environmental conditions throughout the vessel, thereby, allowing for an effective usage of the reactor's total volume leading to optimized and low cost operation (Badkoubi *et al*., 1998; García *et al*., 2005).

Received on January 27, 2019, Accepted on April13, 219Correspondence concerning this article should be addressed to Malek Hajaya (E-mail address: malekhajaya@yahoo.com or mhajaya@ttu.edu.jo).ORCiDID for Malek Hajaya: https://orcid.org/0000-0003-0110-6731

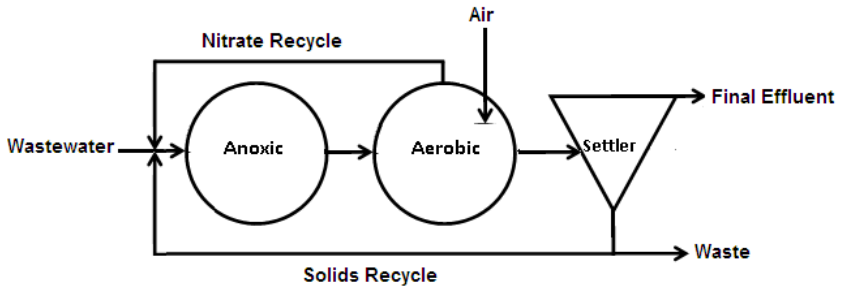

Fig. 1. Typical pre-denitrification activated sludge system including anoxic and aerobic reactors and settler

Despite the assumption of ideal mixing in biological reactors, it is likely non-ideal mixing conditions will prevail in the real situation. Kjellstrand (2006) studied the hydraulic behavior of a denitrifying activated sludge tank, located at the Rya Waste water treatment plant (WWTP) in Göteborg Sweden, where it was found that up to 30% of the feed had notably fast hydraulic retention times, while up to 21% of the feed had notably slow hydraulic retention times compared to the nominal hydraulic retention time. This indicated the presence of feed bypass and stagnation zones in the system. Sánchez and coworkers (Sánchez *et al*., 2016) performed the hydraulic characterization for the secondary treatment system in the WWTP of San Pedro del Pinatar. They reported that only 70.5% of the system's volume was active, while the remaining 29.5% was actually a dead volume.Collivignarelli and coworkers (Collivignarelli *et al*., 2018) reported a dead volume fractions ranging from 15% to 25%, and bypass fractions ranging between 35% and 40%, while performing the experimental verification of reactor hydrodynamics for a undisclosed WWTP. Manenti *and coworkers* (Manenti*et al*., 2018) have identified a 5% fraction of dead volume in a pilot scale WWTP. Non-ideal mixing occurrences in AS systems were reported for constructed, operational wastewater treatment plants, which could be brought by poor design or equipment failure. The cost of diagnosing their presence in such systems could be drastically reduced if mathematical simulations are used. The purpose of this work is to identify the possible consequences of non-ideal mixing on the biological processes performance. Such discrepancies in performance can be used in identifying the presence of non-ideal mixing behavior in the AS system reactors. In this work, a pre-denitrification activated sludge (PD-AS) unit performance with regards to the biological treatment of organic carbon and nitrogen is investigated under the conditions of non-ideal mixing in the anoxic reactor. The system performance is simulated based upon the ASM1 model's biological reactions (Henze *et al*., 2000), and combining two non-ideal mixing two parameter models: CSTR with bypass and dead volume, and two CSTRs with exchange (Fogler, 1999). Performance discrepancies could then be identified by comparing the performance of the system under non-ideal mixing to performance of the system at ideal mixing conditions.

1. Mathematical Models

1.1. Biological Reactions

The ASM1 model identified the specific processes in PD-AS to be: aerobic growth of heterotrophs, anoxic growth of heterotrophs, aerobic growth of autotrophs, decay of heterotrophs, decay of autotrophs, ammonification of soluble organic nitrogen, hydrolysis of entrapped organics, and hydrolysis of entrapped organic nitrogen (Henze *et al*., 2000). **Tables 1** detail each process mathematical model, where *S* denotes the soluble constituents' concentrations, and *X* denotes particulate constituents' concentrations. While **Table 2** lists the different variables associated with the aforementioned processes, with the kinetics of each step involved in the PD-AS system.

1.2 Ideal Completely Mixed Reactors Model

Figure 1 showed the PD-AS system. In this work, both the widely adapted COAST benchmark and BSM1 benchmark(Alex *et al*., 2008; Copp, 2002) are used for system size, albeit with some modifications. The system is designed for an average wastewater flow rate (Q) of 18400m^3/day, with ≈ 300 mg COD/l of biodegradable organic carbon and ≈ 50 mg N/l of nitrogen. Volumes of the anoxic and aerobic reactors are 2000 m^3 (V_1) and 4000 m^3 (V_2), respectively, with nitrate recycle ratio (R_1) and solids recycle ratio (R_2) of 3 and 1, respectively. Waste flow rate (Q_w) is chosen for a 16 day *SRT* to be at 385m^3/day. Air is only introduced into the aerobic reactor to sustain an oxygen concentration of 2.1 ± 0.11 mg/l. The settler sub-model is not included in the system, and it is assumed that no reactions are taking place in it; instead a particulates separation coefficient (*SE*) is assumed and used to calculate the concentration in the settler overflow (final effluent) and underflow. Particulate concentration (X) in both the settler's overflow (X_{OF}) and underflow (X_{UF}) is determined by mass balance around the settler, by using a settling efficiency (*SE*), which is assumed constant (Le Moullec *et al.*, 2011) and can be defined as *SE* = Particulate mass in the underflow/ Particulate mass in the overflow:

$$X_{UF} = [SE.Q.X_2.(R_2+1)]/[R_2.Q+Q_W]\ldots \quad (1)$$
$$X_{OF} = [(1-SE).Q.X_2.(R_2+1)]/[Q+Q_W]\ldots \quad (2)$$

where X_2 is particulate concentration (mg COD/l) in the aerobic reactor.

Table 1. Biological processes taking place in the PD-AS, adapted from the ASM1 model (Henze *et al*., 2000)

Process	Model	Symbol
Aerobic growth of heterotrophs	$\mu_H \frac{S_s}{S_s+K_s}\frac{S_O}{S_O+K_{OH}}X_{BH}$	P_1
Anoxic growth of heterotrophs	$\mu_H \frac{S_s}{S_s+K_s}\frac{K_{OH}}{S_O+K_{OH}}\frac{S_{NO}}{S_{NO}+K_{NO}}\eta_G X_{BH}$	P_2
Aerobic growth of autotrophs	$\mu_A \frac{S_{NH}}{S_{NH}+K_s}\frac{S_O}{S_O+K_{OA}}X_{BA}$	P_3
Decay of heterotrophs	$b_H X_{BH}$	P_4
Decay of autotrophs	$b_A X_{BA}$	P_5
Ammonification of soluble organic nitrogen	$k_a S_{ND} X_{BH}$	P_6
Hydrolysis of entrapped organics	$k_h \frac{X_s/X_{BH}}{X_s/X_{BH}+K_X}\left[\frac{K_{OH}}{S_O+K_{OH}}+\eta_h\frac{S_{NO}}{S_{NO}+K_{NO}}\frac{K_{OH}}{S_O+K_{OH}}\right]X_{BH}$	P_7
Hydrolysis of entrapped organic nitrogen	$P_7\frac{X_{ND}}{X_S}$	P_8

Table 2. State variables in the PD-AS model and their associated rates

Variable	Definition	Rate
S_I[a]	Soluble inert organics	$r_{SI}=0$
S_S[a]	Readily biodegradable (soluble) substrate	$r_{Ss}=\frac{-1}{y_H}(P_1+P_2)+P_7$
X_I[a]	Particulate inert organics	$r_{XI}=0$
X_S[a]	Slowly biodegradable (particulate) substrate	$r_{Xs}=(1-f_P)(P_4+P_5)-P_7$
X_{BH}[a]	Active heterotrophic biomass	$r_{XBH}=P_1+P_2-P_4$
X_{BA}[a]	Active autotrophic biomass	$r_{XBA}=P_3-P_5$
X_P[a]	Non-biodegradable particulates	$r_{Xp}=f_P(P_4+P_5)$
S_O[b]	Dissolved oxygen	$r_{So}=-\frac{1-y_H}{y_H}P_1-\frac{4.57-y_A}{y_A}P_3$
S_{NO}[c]	Nitrate	$r_{SNO}=\frac{1-y_H}{2.86y_H}P_2+\frac{1}{y_A}P_3$
S_{NH}[c]	Free and ionized ammonia	$r_{SNH}=\left(-i_{XB}-\frac{1}{y_A}\right)P_3-i_{XB}(P_1+P_2)+P_6$
S_{ND}[c]	Soluble biodegradable organic nitrogen	$r_{SND}=P_8-P_6$
X_{ND}[c]	Particulate biodegradable organic N	$r_{XND}=(i_{XB}-i_{XP}f_P)(P_4+P_5)-P_8$
S_{ALK}[d]	Alkalinity	$r_{SALK}=P_7\frac{X_{ND}}{X_S}$

a: mg COD/l, mg of Chemical Oxygen Demand; b: mg O_2/ l; c: mg N/ l; d: mol/l.

Assuming ideal CSTR behavior in the anoxic and aerobic reactors, constant liquid densities and reactor volumes, and reactions taking place only in the reactors, the following equations can be used to describe the dynamic behavior of soluble (S) and particulate constituents:

For the anoxic reactor:

$$dS_1/dt = (Q/V_1)\left([S_i+S_2(R_1+R_2)]-[1+R_1+R_2]S_1\right)+r_{S1}\ldots \quad (3)$$
$$dX_1/dt = (Q/V_1)\left([X_i+X_2R_1+X_{UF}R_2]-[1+R_1+R_2]X_1\right)+r_{X1}\ldots \quad (4)$$

For the aerobic reactor:

$$dS_2/dt = (Q[1+R_1+R_2]/V_2)\,(S_1-S_2)+r_{S2}\ldots \quad (5)$$
$$dX_2/dt = (Q[1+R_1+R_2]/V_2)\,(X_1-X_2)+r_{X2}\ldots \quad (6)$$

where S_1 and X_1 are the concentrations in the anoxic reactor, $S_i$and X_i are the concentrations in the feed wastewater (Table 3), and S_2 and X_2 are the concentrations in the aerobic reactor, respectively. X_{UF} is the particulate concentrations in the solids recycle (Equation 1), and $r_{S1\&S2}$ and $r_{X1\&X2}$ are the rates in the different reactors (Table 2). Finally for oxygen, in the aerobic reactor, the following rate is introduced to represent the aeration rate ($r_{Air\text{-}in}$):

$$r_{Air-in} = K_L(S_O^{SAT} - S_{O2})\ldots \quad (7)$$

where K_L is the oxygen transfer coefficient (d^{-1}) maintained at a level in the aerobic reactor to provide a constant oxygen concentration (as mentioned above)(Alex *et al*., 2008), and S_O^{SAT} is oxygen saturation concentration = 8 mg/l, (at 26°C and 1atm) (Rittmann and McCarty, 2001), and S_{O2} in the oxygen concentration in the aerobic reactor (mg/l).

1.3 Non-ideal Mixing Models

Among the PD-AS system reactors, the anoxic reactor is the most susceptible to the occurrence of non-ideal mixing. Mixing in this reactor is solely performed mechanically, compared to superior mixing conditions (minimizing non-ideal mixing) brought by the aeration process taking place in the aerobic reactor. Accordingly, the non ideal mixing scenarios are assumed to affect the anoxic reactor in the PD-AS. Oxygen concentration and settler behavior are handled in the same matter as discussed above in the ideal CSTR based system.

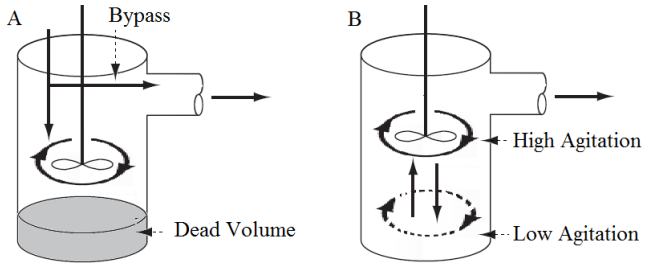

Fig. 2. Non ideal, real mixing scenarios; A: Bypass with dead volume, and B: Rapid and slow mixing.

1.3.1 CSTR with bypass and dead volume

In this situation, poor mixing results in generating a dead zone within the reactor volume, where limited or no exchange of material is taking place between it and the remaining reactor volume. This will reduce the available volume for reactions within the reactor itself. In addition, poor mixing can allow for a portion of the feed to exit rapidly without being mixed inside the reactor, as if that portion is totally not entering the reactor, but rather bypassing it directly to the effluent (Figure 2.A). Previous scenarios are modeled as a combination of an ideal CSTR coupled with a dead zone. These volumes are defined as fractions of the total reactor volume (*V*), where α = *volume of CSTR*/*V* and (1-α) = *volume of dead zone*/*V*. On the other hand, flow rates headed for the reactor (*Q*) have a fraction that bypasses it while the remaining fraction enters it, where β= *bypassed flow*/*Q* and (1-β)= *entering flow*/*Q* (Fogler, 1999). The degree of non ideality depends on values of α and β. The presence of a bypass and a dead volume in real, engineered biological reactors has been previously reported (Collivignarelli *et al*., 2018; Kjellstrand, 2006; Manenti *et al*., 2018; Sánchez *et al*., 2016).
In the light of the previous argument, the dynamic behavior of soluble and particulate constituents in both reactors no longer behaves as described by Equations 3, 4, 5, and 6. Assuming constant values for α, β (for all streams entering), liquid densities and reactor volumes, and reactions taking place only in the reactors, the following equations can be used to describe the dynamic behavior of soluble and particulate constituents:
For the anoxic reactor:

$$dS_1/dt = (Q(1-\beta)/\alpha V_1)\,([S_i + S_2(R_1+R_2)] - [1+R_1+R_2]S_1) + r_{S1}\ldots \quad (8)$$

$$dX_1/dt = (Q(1-\beta)/\alpha V_1)\,([X_i + X_2R_1 + X_{UF}R_2] - [1+R_1+R_2]X_1) + r_{X1}\ldots \quad (9)$$

For the aerobic reactor:

$$dS_2/dt = (Q/V_2)\left((1-\beta)[1+R_1+R_2]S_1 + \beta[S_i + S_2(R_1+R_2)] - [1+R_1+R_2]S_2\right) + r_{S2}\ldots \quad (10)$$

$$dX_2/dt = (Q/V_2)\left((1-\beta)[1+R_1+R_2]X_1 + \beta[X_i + X_2R_1 + X_{UF}R_2] - [1+R_1+R_2]X_2\right) + r_{X2}\ldots \quad (11)$$

1.3.2 Two CSTRs with material exchange

This scenario depicts a situation where mixing apparatus are poorly situated within the reactor, resulting in rapid mixing in their vicinity, while the remaining region undergoes mixing, albeit in a lesser rate. This situation will influence the distribution of material within the reactor, affecting the different reactions rates due to an uneven distribution of substrates (Figure 2.B). In this situation, it is assumed that the anoxic reactor volume (*V*) is split into two fractions: a fraction that undergoes high agitation (α = highly agitated volume/*V*) and a fraction with low agitation ((1-α) = volume with less agitation/*V*). Material is exchanged between the two volume fractions by a ratio of the flows entering the reactor; β= material exchange flow rate/*Q*. Both the inlet and outlet flow is directed to and from the highly agitated portion (Fogler, 1999). As with the previous model, the degree of non ideality depends on values of α and β.

The two CSTR with exchange model has been previously used to describe non ideal mixing in different biological reactors (Le Moullec *et al.*, 2010;Le Moullec *et al.*, 2011;Pereira *et al.*, 2012). Assuming constant values for α, β (for all streams entering), liquid densities and reactor volumes, and reactions taking place only in the reactors, the following equations can be used to describe the dynamic behavior of soluble and particulate constituents:

For the anoxic reactor highly agitated fraction (concentrations are accented with 1):

$$dS^1{}_1/dt = (Q(1+R_1+R_2)/\alpha V_1)\left([S_i + S_2(R_1+R_2)/1+R_1+R_2] - S^1{}_1 + \beta(S^2{}_1 - S^1{}_1)\right) + r_{S_1^1}\ldots \quad (12)$$

$$dX^1{}_1/dt = (Q(1+R_1+R_2)/\alpha V_1)\left([X_i + X_2R_1 + X_{UF}R_2)/1+R_1+R_2] - X^1{}_1 + \beta(X^2{}_1 - X^1{}_1)\right) + r_{X_1^1}\ldots \quad (13)$$

For the anoxic reactor fraction with less agitated (concentrations are accented with 2):

$$dS^2{}_1/dt = (Q(1+R_1+R_2)\beta/(1-\alpha)V_1)\,(S^1{}_1 - S^2{}_1) + r_{S_1^2}\ldots \quad (14)$$

$$dX^1{}_1/dt = (Q(1+R_1+R_2)\beta/(1-\alpha)V_1)\,(X^1{}_1 - X^2{}_1) + r_{X_1^2}\ldots \quad (15)$$

For the aerobic reactor:

$$dS_2/dt = (Q(1+R_1+R_2)/V_2)\,(S^1{}_1 - S_2) + r_{S2}\ldots \quad (16)$$

$$dX_2/dt = (Q(1+R_1+R_2)/V_2)\,(X^1{}_1 - X_2) + r_{X2}\ldots \quad (17)$$

2. Computer Simulations

The performance of the PD-AS is simulated dynamically under ideal conditions (CSTR) and real conditions (CSTR with dead volume and two CSTRs with material exchange). The characteristics of treated wastewater are given in **Table 3**, and the kinetic and stoichiometric parameters are given in **Table 4**.

Table 3. Wastewater characteristics used in the simulations (Vanhooren and Nguyen, 1996).

Variable	Value
S_{Ii}[a]	30
S_{Si}[a]	70
X_{Ii}[a]	52
X_{Si}[a]	200
X_{BHi}[a]	28
X_{BAi}[a]	0.25
X_{Pi}[a]	5.0
S_{Oi}[b]	0.25
S_{NOi}[c]	0.25
S_{NHi}[c]	30.0
S_{NDi}[c]	7.0
X_{NDi}[c]	11.0
S_{ALKi}[d]	10.0

a: mg COD/l, mg of Chemical Oxygen Demand; b: mg O_2/ l; c: mg N/ l; d: mol/l.

The group of ODEs representing the behavior of all constituents in the system where solved simultaneously in order to simulate the operation of the system for 30 days. The equations were solved using fourth-order Runge–Kutta procedure in MATLAB (The MathWorks Inc., Natick, MA), with a maximum time step of 1 day. The system's performance was evaluated by calculating the following constituents in the effluent (Alex *et al*., 2008):

A. Total Kjeldahl Nitrogen (Rittmann and McCarty, 2001) in effluent and waste (TKN_E and TKN_W):

$$TKN_E = S_{NH}^2 + X_{ND}^{OF} + i_{XB}(X_{BA}^{OF} + X_{BH}^{OF}) + i_{XP}(X_P^{OF} + X_I^{OF})\ldots \quad (18)$$

$$TKN_W = S_{NH}^2 + X_{ND}^{UF} + i_{XB}(X_{BA}^{UF} + X_{BH}^{UF}) + i_{XP}(X_P^{UF} + X_I^{UF})\ldots \quad (19)$$

B. Total Ammonia and Nitrate concentrations ($S_{NH\text{-}E}$ and $S_{NO\text{-}E}$).

C. Biochemical oxygen demanding (Rittmann and McCarty, 2001) organics in effluent (BOD_E and BOD_W):

$$BOD_E = 0.25\left(S_S^2 + X_S^{OF} + (1-f)(X_{BA}^{OF} + X_{BH}^{OF})\right) \quad (20)$$

$$BOD_W = 0.25\left(S_S^2 + X_S^{UF} + (1-f)(X_{BA}^{UF} + X_{BH}^{UF})\right) \quad \ldots(21)$$

D. Chemical oxygen demanding (Rittmann and McCarty, 2001) organics in effluent and waste (COD_E and COD_W):

$$COD_E = S_I^2 + S_S^2 + X_I^{OF} + X_S^{OF} + X_{BA}^{OF} + X_{BH}^{OF} + X_P^{OF} \quad (22)$$

$$COD_W = S_I^2 + S_S^2 + X_I^{UF} + X_S^{UF} + X_{BA}^{UF} + X_{BH}^{UF} + X_P^{UF}\ldots \quad (23)$$

To study the system performance under real conditions, multiple simulations were performed while varying the values of the two parameters in the real reactor models in order to reflect varying degrees of non ideal flow: For the CSTR with dead volume model, α was changed from 1 to 0.1, while β was changed from 0 to 0.9, and for the two CSTRs with exchange model α was changed from 0.9 to 0.1, while β was changed from 0.01 to 0.9. The aforementioned values for α and β were chosen to depict a moderate, intermediate, and extreme non ideal flow scenarios.

Table 4.Kinetic and stoichiometric parameters used in the simulation (Alex *et al*., 2008)

Parameter	Definition	Value
μ_H	Max. specific growth rate for Heterotrophs (d^{-1})	4.0
μ_A	Max. specific growth rate for Autotrophs (d^{-1})	0.5
K_S	Half saturation constant for Heterotrophs (mg COD/l)	10
K_{OH}	Half saturation constant for O_2 Heterotrophs (mg O_2/l)	0.2
K_{NO}	Half saturation constant for Heterotrophs (mg NO_3-N/l)	0.5
η_G	Correction for Anoxic Heterotrophic growth (-)	0.8
K_{OA}	Half saturation constant for O_2 Autotrophs (mg O_2/l)	0.4
K_{NH}	Half saturation constant for Autotrophic. (mg NH_3-N/l)	1.0
b_H	Decay constant for Heterotrophs (d^{-1})	0.3
b_A	Decay constant for Autotrophs (d^{-1})	0.05
k_a	Ammonification rate (l.COD/mg.d)	0.05
k_h	Max. specific Hydrolysis rate (mg COD/mg COD biomass.d)	3.0
K_X	Half saturation constant for Hydrolysis (mg COD/mg COD biomass)	0.1
η_h	Correction for Anoxic Hydrolysis (-)	0.8
y_H	Heterotrophic yield coefficient (mg biomass/mg COD)	0.67
y_A	Autotrophic yield coefficient (mg biomass/mg N)	0.24
f_p	Particulate yielding biomass fraction (-)	0.08
i_{XB}	Nitrogen fraction in biomass (mg N/mg COD biomass)	0.08
i_{XP}	Nitrogen fraction in biomass products (mg N/mg COD biomass)	0.06

3 Results and Discussion

3.1 Ideal Completely Mixed Reactors

The PD-AS system operation was simulated for 30 days. **Figure 3** shows the system performance as a function of time.

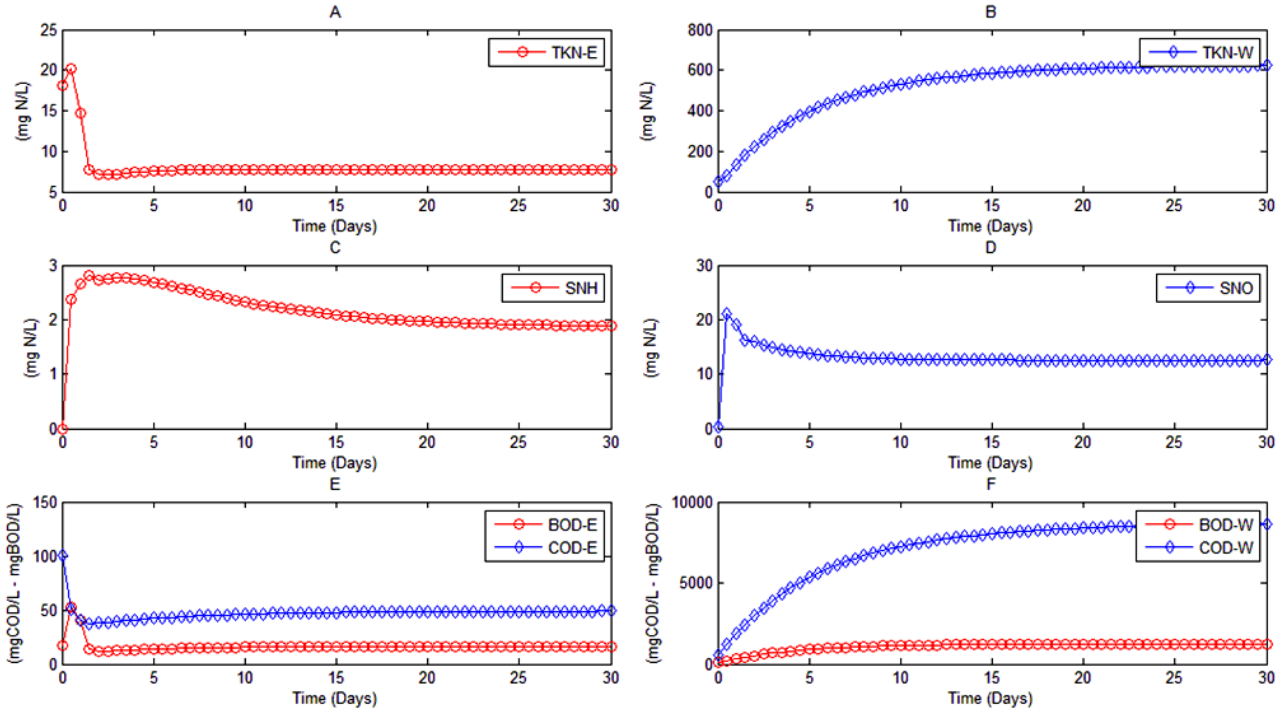

Fig. 3. PD-AS performance under ideal mixing condition; A: TKN_E, B: TKN_W, C: $S_{NH\text{-}E}$, D: $S_{NO\text{-}E}$, E: BOD_E and COD_E, and F: BOD_W and COD_W.

Effluent steady state S_{NH} , S_{NO}, and TKN_E concentrations were 1.8, 12.5, and 3.9 mg N/l, respectively, while BOD_E and COD_E were 16.4 mg/l and 48.9 mg/l, respectively. The daily waste included 626 mg N/l of *TKN* , 1271 mg/L of BOD, and 8625 mg/L of COD. The simulation outcome was comparable to other published simulations results for similar PD-AS reactor sizes and feed wastewater composition (Alex *et al*., 2008).

3.2 CSTR with bypass and dead volume:

Figure 4 shows the effect of varying the non ideal mixing parameters on the concentration of nitrogen compounds in the system. As it can be seen, the system's effluent TKN concentration varied marginally with increasing mixing non idealities (**Figure 4.A**) (i.e. increased bypass fraction and dead volume fraction). This can be attributed to the fact that effluent TKN is mainly soluble, and

removed in the aerobic reactor, where mixing performance was assumed ideal.

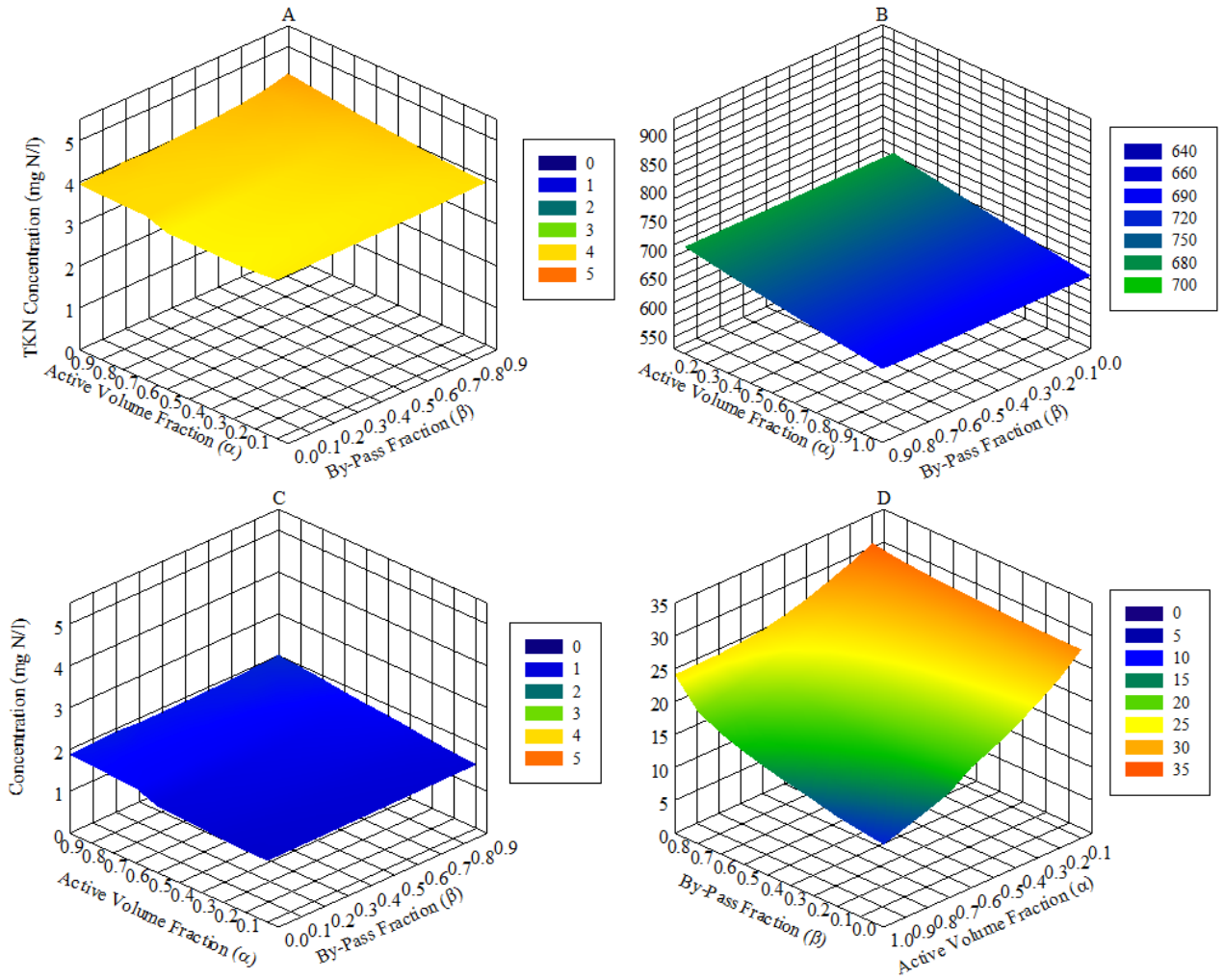

Fig.4: Simulated PD-AS nitrogen related performance under CSTR with bypass/dead volume non ideal mixing effects at $0.1 \leq \alpha \leq 1.0$ and$0 \leq \beta < 0.9$; A: TKN_E, B: TKN_W, C: $S_{NH\text{-}E}$, and D: $S_{NO\text{-}E}$.

The same trend was noticed for the total ammonia in the effluent, which remained relatively constant (**Figure 4.C**). TKN_W increased with increasing mixing non idealities, as it can be seen in **Figure 4.B.** This is attributed by the increase in the heterotrophic biomass in the system (from 2570 to 2980 mg COD/l) as a result to the increase in substrate availability in the aerobic reactor brought by the increase in bypass ratio. The TKN_W increase may affect anaerobic treatment for the wasted biomass (Chen *et al*., 2008; Tezel *et al*., 2014), due to the elevated levels of nitrogen. On the other hand, the effluent nitrate concentration increased drastically as the system was shifted towards non ideal mixing conditions. As seen in Figure 4.C, $S_{NO\text{-}E}$ exceeded 20 mg N/l at $\alpha \leq 0.4$ and $\beta \leq 0.4$. The decrease inα (increase in dead volume fraction) had a larger effect on $S_{NO\text{-}E}$ compared to β. Similar performance short comes were observed by Manenti*et al*. (Manenti*et al*., 2018), when the actual retention time failed in assuring an acceptable treatment level below a minimum threshold value. Collivignarelli*et al*.(Collivignarelli*et al*., 2018) reported that reducing the dead volume fraction will result in an enhancement of nitrate removal, while Kjellstr and and co-researchers (Kjellstrand*et al*., 2005) reported that the presence of a dead volume in the reactor will reduce the denitrifying capacity due to reduced active volume, and high nitrate concentration in the effluent can appear due to the short circuiting stream (bypass). **Figure 5** shows the effect of varying the non ideal mixing parameters on the concentration of BOD and COD in the system. As seen in **Figure 5.A** and **Figure 5.B**, increasing mixing non idealities had a slight effect on BOD_E and COD_E. However, as with $S_{NO\text{-}E}$, decreasing α had the main effect. This can be attributed to the reduction in the anoxic reactor active volume size, leading to a lesser conversion due to smaller real retention times (Fogler, 1999). This connects to the increase in $S_{NO\text{-}E}$ as seen in Figure 4.D, since (as mentioned in section 1) nitrite is utilized exclusively by the heterotrophic biomass organic carbon mineralization in the anoxic reactor.

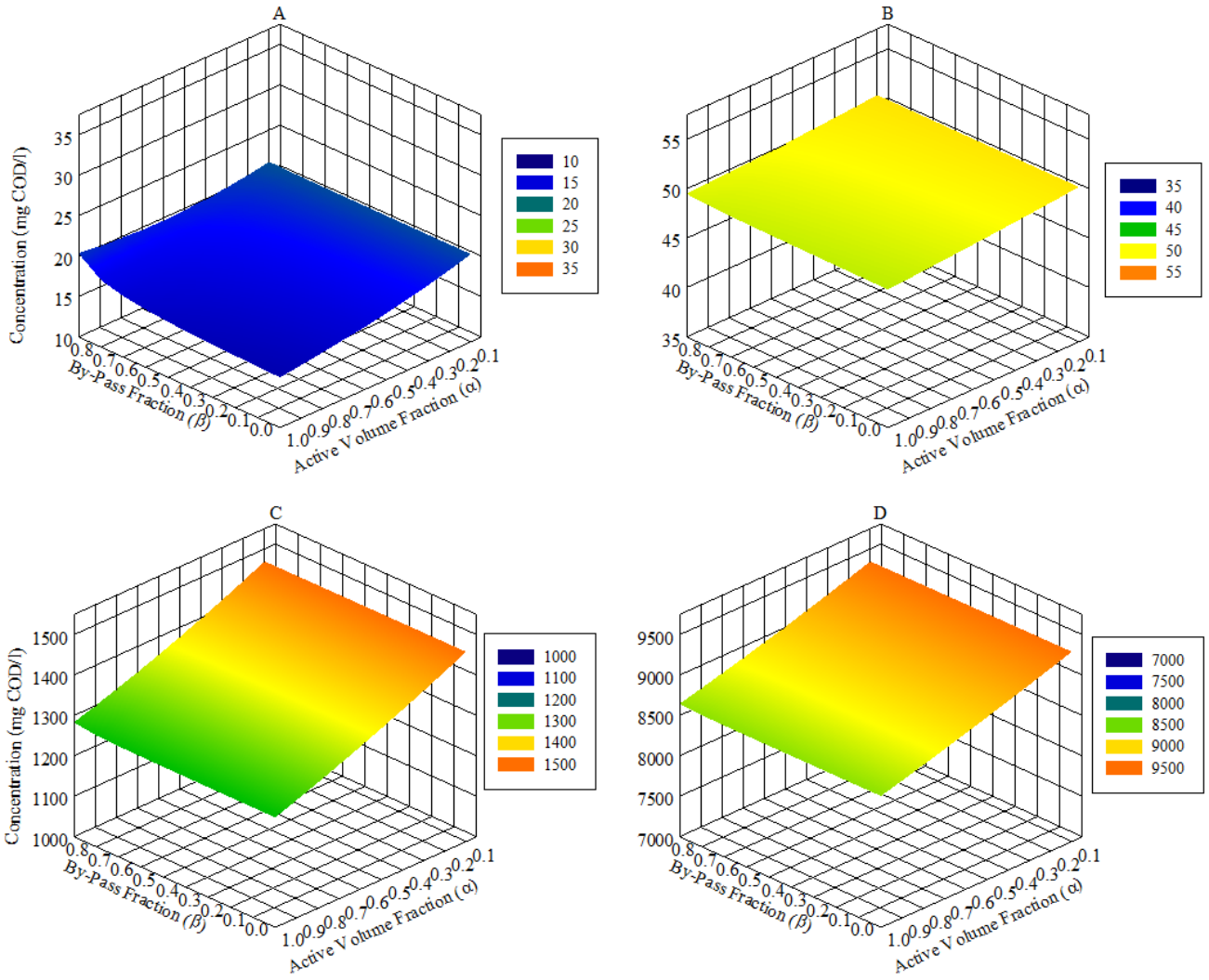

Fig. 5.Simulated PD-ASorganic carbon related performanceunder CSTR with bypass/dead volume non ideal mixing effectsat $0.1 \leq \alpha \leq 1.0$ and$0 \leq \beta < 0.9$; A: BOD_E, B: COD_E, C: BOD_W, and D: COD_W.

As seen in Figure 5.C and Figure 5.D, both of BOD_W and COD_W concentrations increased in the waste stream as a direct response to increased biomass in the system, which was brought by the greater than before availability of substrate in the aerobic reactor due to increased bypass fraction and decreased active volume fraction in the anoxic reactor. Collivignarelli *et al.* (Collivignarelli *et al*., 2018) reported that reducing the dead volume fraction will enhance COD and BOD. The increase in the concentrations of BOD_W and COD_W in the waste stream, coupled with the increase of TKN_W, will amplify the load on waste disposal facilities in the wastewater treatment plant. Similar to what have been observed with $S_{NO\text{-}E}$ above, the active volume fraction (α) had a larger effect on the system's *BOD* and *COD* concentrations when compared to the bypass fraction. It must be added that, apart from nitrate concentration, the resulting changes in the PD-AS's performance were related to particulate constituents in the system. However, their concentration in the system is directly correlated with the settler's performance (i.e. *SE* value). The SE value was assumed constant to eliminate the effect of the settler's performance on the predicted outcome.

3.3 Two CSTRs with material exchange

As mentioned in section 2.3.2, this model describes a scenario where the mixing apparatus in the anoxic reactor are poorly positioned, resulting in rapid mixing in their vicinity, while the remaining region undergoes mixing, albeit in a lesser rate. Carried out simulations for the system's operation at the current non-ideal mixing scenario showed that, to some extent, its performance was unaffected. This was in a specific range of the mixing model α and β values: $0.4 \leq \alpha \leq 0.9$ and$0.1 \leq \beta \leq 0.9$. Table 5 shows the unaffected system's performance. **Figure 6 and Figure 7** shows the systems performance beyond the abovementioned range for the mixing model parameters values (i.e. 2nd range at $0.1 \leq \alpha < 0.4$ and$0.01 \leq \beta < 0.1$). It is clear that the system's effluent TKN concentration slightly (**Figure 6.A**)varied with increasing mixing non idealities within the 2nd range (i.e. reducing the rapid agitation zone and material exchange fractions). This took place because *TKN* is mainly removed in the aerobic reactor, which its mixing performance was assumed ideal. The relatively constant total ammonia in the effluent (**Figure 6.C**) suggests that that ammonia removal is unaffected.

Table 5. Effluent Constituents of the PD-AS system with and without ideal mixing conditions

Effluent Constituents	Ideal mixing	CSTRs with material exchange
TKN_E	3.9 mg N/l	3.9±0.09[a]mg N/l
TKN_W	626.5 mg N/l	628.5±4.8mg N/l
$S_{NH\text{-}E}$	1.9 mg N/l	1.8±0.05mg N/l
$S_{NO\text{-}E}$	12.6 mg N/l	14.1±1.2mg N/l
BOD_E	16.2 mg BOD/l	16.7±0.9 mg BOD/l
COD_E	48.9 mg COD/l	49.1±0.2 mg COD/l
BOD_W	1271.9 mg BOD/l	1278.8±15.2 mg BOD/l
COD_W	8625.6 mg COD/l	8652.3±61.5 mg COD/l

a: Average ± Standard Deviation.

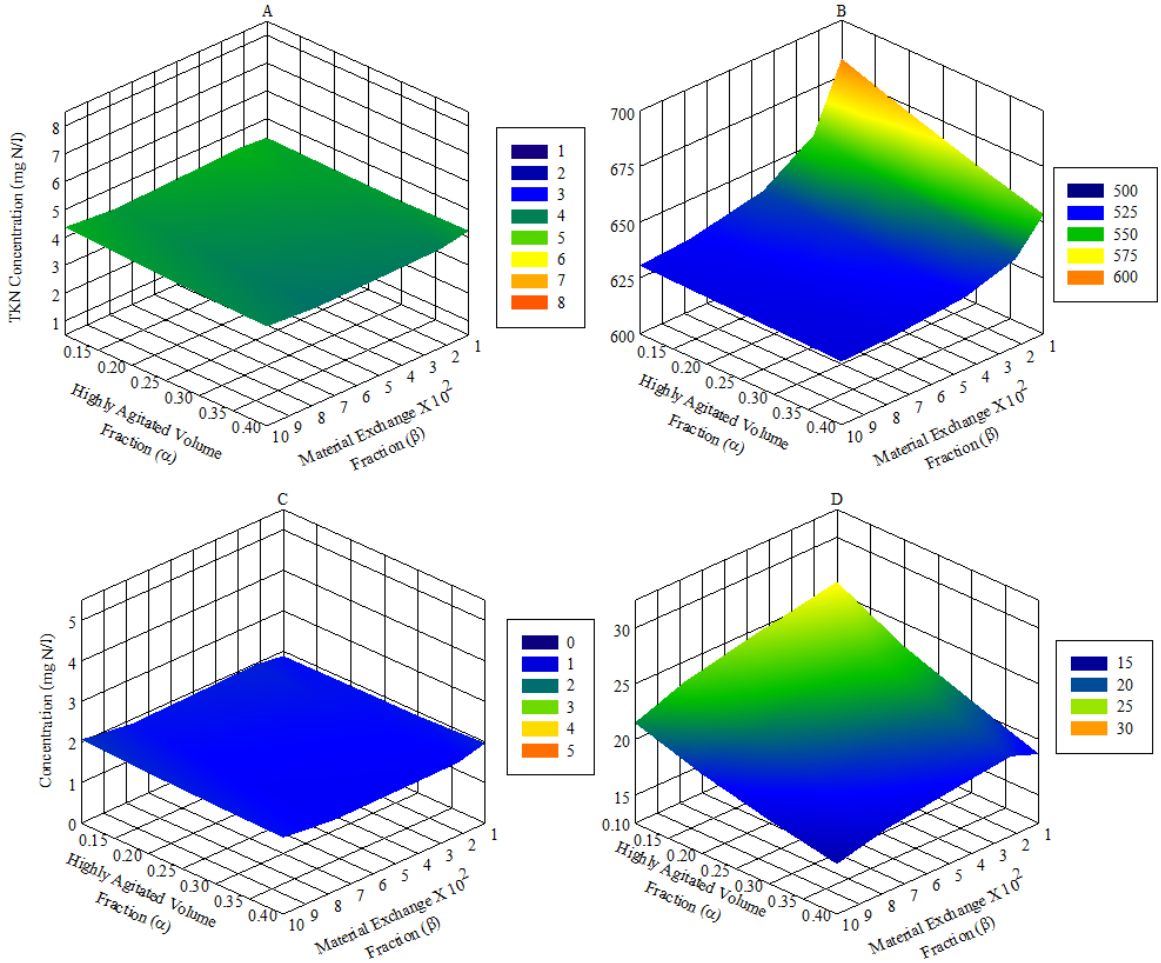

Fig. 6. Simulated PD-AS nitrogen related performanceunder the 2 CSTRs with material exchange non ideal mixing effects at $0.1 \leq \alpha < 0.4$ and$0.01 \leq \beta < 0.1$; A: TKN_E, B: TKN_W, C: $S_{NH\text{-}E}$, and D: $S_{NO\text{-}E}$.

However, the TKN_W (which is mainly comprised from particulates) increased with increasing mixing non idealities (**Figure 6.B**), but only at extreme non-ideal mixing condition, when the anoxic reactor volume was mostly affected by low mixing due very slow agitation ($\alpha < 0.3$ and $\beta < 0.01$). Operation within this range also increased the heterotrophic biomass in the system (from 2570 to 2708±136 mg COD/l), due to ineffective utilization of readily biodegradable organic carbon in the anoxic reactor ($S_S + X_S$ increased in the anoxic reactor effluent from 82.2 to 117±12 mg COD/l), and were utilized by the aerobic reactor. Similar to the dead volume/bypass model, the increase TKN_W concentration and biomass concentration in the waste stream may affect anaerobic treatment

processes for the wasted biomass. The effluent nitrate concentration increased drastically as the system was shifted towards extreme non-ideal mixing conditions. As seen in Figure 6.C, $S_{NO\text{-}E}$ exceeded 20 mg N/l at $\alpha < 0.2$ and $\beta < 0.01$. This behavior mimicked the result seen in the dead volume/bypass model, however at more extreme non-ideal mixing conditions in this model. The increase is probably a result of the anoxic reactor active volume becoming extremely low (i.e. fast residence times), not permitting any effective reactions. This can be connected to the increase of readily biodegradable organic carbon in the anoxic reactor (see before), being not utilized fully under these conditions. Results shown in Fig. 6 showed that the system's performance was more affected by the high agitation fraction (α).Fig. 7 shows the effect of varying the non ideal mixing parameters on the concentration of BOD and COD in the system.

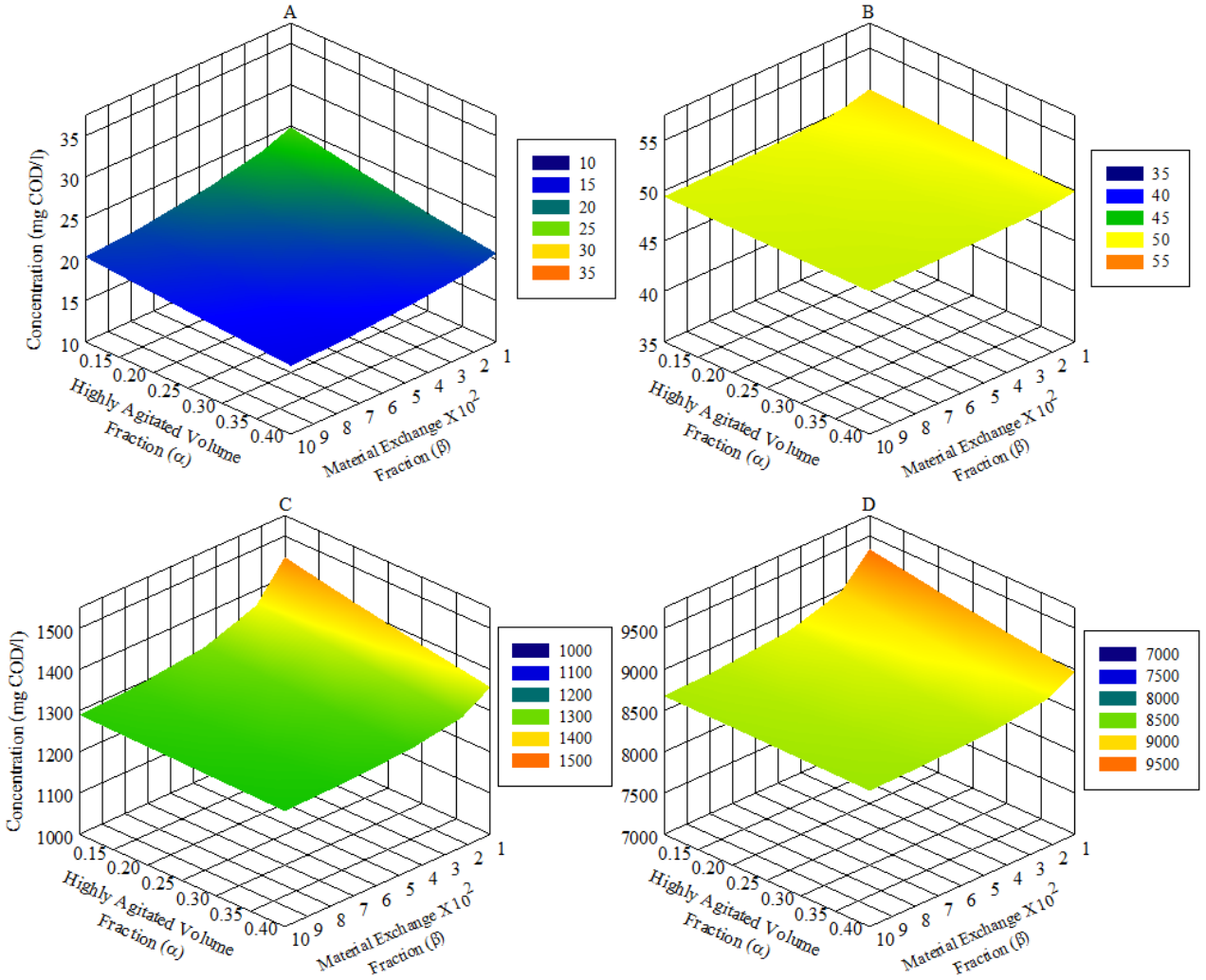

Fig. 7. Simulated PD-AS nitrogen related performanceunder the 2 CSTRs with material exchange non ideal mixing effects at $0.1 \leq \alpha < 0.4$ and$0.01 \leq \beta < 0.1$; A: TKN_E, B: TKN_W, C: $S_{NH\text{-}E}$, and D: $S_{NO\text{-}E}$.

As seen in Fig. 7.A and Fig. 7.B, only extreme levels of mixing non idealities had an effect on BOD_E and COD_E. The increase is probably related to the increased heterotrophic biomass in the system (from 2570 to 2708±136 mg COD/l), due to ineffective utilization of readily biodegradable organic carbon in the anoxic reactor. As seen in Fig. 7.C and Fig. 7.D, both of BOD_W and COD_W concentrations increased in the waste stream as a direct response to increased biomass in the system, which was brought by the greater than before availability of substrate in the aerobic reactor due reduced active anoxic reactor volume. The increase in the concentrations of BOD_W and COD_W in the waste stream will amplify the load on waste disposal facilities in the wastewater treatment plant. Aforementioned results showed that the system's performance was more affected by the high agitation fraction (α). Results shown in Figs. 6 and**7** showed that the non-ideal mixing scenario depicted by the two CSTRs with material exchange, had minor effects on the performance of the PD-AS system. Even so, these effects occurred at extreme non-ideal situations. However, this stipulation could be related to the specific operational conditions of the PD-AS under investigation. Moreover, previously published work suggests that increasing the number of CSTRs (i.e. compartments) in this model could provide a more representative depiction of the mixing non-idealities in AS systems (Liotta *et al.*, 2014).

Conclusions

The system's performance was largely affected by the presence of a dead volume/bypass scenario compared to the two mixing zones with material exchange scenario. Under non-ideal mixing conditions, effluent concentrations of Total Kjeldahl Nitrogen, organic carbon increased marginally. On the other hand, the effluent concentration of nitrate increased significantly under the same conditions, indicating a reduction in nitrate removal efficiency. The heterotrophic biomass concentration in the system increased under non-ideal mixing conditions. This by its part resulted in an increase in the waste stream concentrations of Total Kjeldahl Nitrogen and organic carbon. This study provides an insight on the behavior of pre-denitrification activated sludge systems when affected by non-ideal mixing conditions. Additionally, it identified some performance discrepancies that could-if found in a real system-indicate the presence of a dead volume/bypass or two mixing zones mixing non-idealities in the anoxic reactor.

Nomenclature

Acronyms

AS:	Activated Sludge
PD:	Pre-Denitrification
CSTR:	Continuous stirred-tank reactor
SE:	particulates separation coefficient
COD:	Chemical Oxygen Demand
BOD:	Biochemical Oxygen Demand
TKN:	Total Kjeldahl Nitrogen
E:	Effluent
W:	Waste
UF:	Underflow
OF:	Overflow

Symbols

S:	Dissolved material concentration	[mg COD/l]
S_i:	Dissolved material concentration in the feed	[mg COD/l]
S_I:	Soluble inert organics concentration	[mg COD/l]
S_S:	Readily biodegradable (soluble) substrate concentration	[mg COD/l]
X:	particulate material concentration	[mg COD/l]
X_i:	Particulate material concentration in the feed	[mg COD/l]
X_I:	Particulate inert organics concentration	[mg COD/l]
X_S:	Slowly biodegradable (particulate) concentration	[mg COD/l]
X_{BH}:	Active heterotrophic biomass concentration	[mg COD/l]
X_{BA}:	Active autotrophic biomass concentration	[mg COD/l]
X_P:	Non-biodegradable particulates from cell decay concentration	[mg COD/l]
S_O:	Dissolved oxygen concentration	[mg O_2/l]
S_O^{SAT}:	Saturation dissolved oxygen concentration	[mg O_2/l]
S_{NO}:	Nitrate concentration	[mg N/l]
S_{NH}:	Free and ionized ammonia concentration	[mg N/l]
S_{ND}:	Soluble biodegradable organic nitrogen concentration	[mg N/l]
X_{ND}:	Particulate biodegradable organic nitrogen concentration	[mg N/l]
S_{ALK}:	Alkalinity	[mol/l]
K_L:	oxygen transfer coefficient	[d^{-1}]
Q:	Feed wastewater flow rate	[m^3/d]
Q_W:	Waste flow rate	[m^3/d]
R_1:	Nitrate recycle ratio	[-]
R_2:	Solids recycle ratio	[-]
V_1:	Anoxic reactor volume	[m^3]
V_2:	Aerobic reactor volume	[m^3]
r:	Reaction rate	[mg/l.d]
K_S:	Half saturation constant for Heterotrophs ()	[mg COD/l]
K_{OH}:	Half saturation constant for O_2 Heterotrophs (mg O_2/l)	[mg O_2/l]
K_{NO}:	Half saturation constant for Heterotrophs (mg NO_3-N/l)	[mg NO_3-N/l]
K_{OA}:	Half saturation constant for O_2 Autotrophs (mg O_2/l)	[mg O_2/l]
K_{NH}:	Half saturation constant for Autotrophic. (mg NH_3-N/l)	[mg NH_3-N/l]
b_H:	Decay constant for Heterotrophs (d^{-1})	[d^{-1}]
b_A:	Decay constant for Autotrophs (d^{-1})	[d^{-1}]
k_a:	Ammonification rate (l.COD/mg.d)	[l.mg COD/mg.d]
k_h:	Max. specific Hydrolysis rate (mg COD/mg COD biomass.d)	[mg COD/mg COD.d]
K_X:	Half saturation constant for Hydrolysis (mg COD/mg COD biomass)	[mg COD/mg COD]
y_H:	Heterotrophic yield coefficient (mg biomass/mg COD)	[mg biomass/mg COD]
y_A:	Autotrophic yield coefficient (mg biomass/mg N)	[mg biomass/mg N]
f_p:	Particulate yielding biomass fraction (-)	[-]
i_{XB}:	Nitrogen fraction in biomass (mg N/mg COD biomass)	[mg N/mg COD biomass]
i_{XP}:	Nitrogen fraction in biomass products (mg N/mg COD biomass)	[mg N/mg COD biomass]

Greek letters

α:	Non-ideal mixing parameter 1	[-]
β:	Non-ideal mixing parameter 2	[-]
μ_H:	Max. specific growth rate for Heterotrophs (d^{-1})	[d^{-1}]
μ_A:	Max. specific growth rate for Autotrophs (d^{-1})	[d^{-1}]
η_G:	Correction for Anoxic Heterotrophic growth (-)	[-]
η_h:	Correction for Anoxic Hydrolysis (-)	[-]

References

Alex, J., Benedetti, L., Copp, J., Gernaey, K., Jeppsson, U., Nopens, I., Pons, M., Rieger, L., Rosen, C. and Steyer, J. "Benchmark simulation model no. 1 (bsm1)", *Report by the IWA Taskgroup on Benchmarking of Control Strategies for WWTPs*, (2008).

Badkoubi, A., Ganjidoust, H., Ghaderi, A. and Rajabi, A. "Performance of a subsurface constructed wetland in iran", *Water Science and Technology*, **38**, 345-350, (1998).

Chen, Y., Cheng, J. J. and Creamer, K. S. "Inhibition of anaerobic digestion process: A review", *Bioresource Technology*, **99**, 4044-4064, (2008).

Collivignarelli, M., Bertanza, G., Abbà, A. and Damiani, S. "Troubleshooting in a full-scale wastewater treatment plant: What can be learnt from tracer tests", *International Journal of Environmental Science and Technology*, 1-12, (2018).

Copp, J. B.; "The cost simulation benchmark: Description and simulator manual: A product of cost action 624 and cost action 682", *EUR-OP*, (2002).

Fogler, H. S.; "Elements of chemical reaction engineering", Upper Saddle River, New Jersey, *Pearson Education, Inc.*, (1999).

García, J., Aguirre, P., Barragán, J., Mujeriego, R., Matamoros, V. and Bayona, J.M. "Effect of key design parameters on the efficiency of horizontal subsurface flow constructed wetlands", *Ecological Engineering*, **25**, 405-418, (2005).

Hajaya, M.G. and Pavlostathis, S.G. "Modeling the fate and effect of benzalkonium chlorides in a continuous-flow biological nitrogen removal system treating poultry processing wastewater", *Bioresource Technology*, **130**, 278-287, (2013).

Hellinga, C., van Loosdrecht, M. and Heijnen, J.J. "Model based design of a novel process for nitrogen removal from concentrated flows", *Mathematical and Computer Modelling of Dynamical Systems*, **5**, 351-371, (1999).

Henze, M., Gujer, W., Mino, T. and van Loosdrecht, M.C.; "Activated sludge models asm1, asm2, asm2d and asm3", *IWA publishing*, (2000).

Kim, H., Noh, S. and Colosimo, M. "Modeling a bench-scale alternating aerobic/anoxic activated sludge system for nitrogen removal using a modified asm1", *Journal of Environmental Science and Health Part a-Toxic/Hazardous Substances & Environmental Engineering*, **44**, 744-751, (2009).

Kjellstrand, R. "Hydraulic behaviour in an activated sludge tank: From tracer test through hydraulic modelling to full-scale implementation" [Dissertation], Göteborg: Chalmers tekniska högskola, (2006)

Kjellstrand, R., Mattsson, A., Niklasson, C. and Taherzadeh, M.J. "Short circuiting in a denitrifying activated sludge tank", *Water Science and Technology*, **52**, 79-87, (2005).

Le Moullec, Y., Gentric, C., Potier, O. and Leclerc, J. "Comparison of systemic, compartmental and cfd modelling approaches: Application to the simulation of a biological reactor of wastewater treatment", *Chemical Engineering Science*, **65**, 343-350, (2010).

Le Moullec, Y., Potier, O., Gentric, C. and Leclerc, J. "Activated sludge pilot plant: Comparison between experimental and predicted concentration profiles using three different modelling approaches", *Water Research*, **45**, 3085-3097, (2011).

Liotta, F., Chatellier, P., Esposito, G., Fabbricino, M., Van Hullebusch, E.D. and Lens, P.N. "Hydrodynamic mathematical modelling of aerobic plug flow and nonideal flow reactors: A critical and historical review", *Critical Reviews in Environmental Science and Technology*, **44**, 2642-2673, (2014).

Madigan, M. T. and Martinko, J. M.; "Brock biology of microorganisms ", Upper Saddle River, NJ, *Pearson Prentice Hall*, (2006).

Manenti, S., Todeschini, S., Collivignarelli, M.C. and Abbà, A. "Integrated rtd− cfd hydrodynamic analysis for performance assessment of activated sludge reactors", *Environmental Processes*, 1-20, (2018).

Ostace, G. S., Cristea, V. M. and Agachi, P. Ş. "Cost reduction of the wastewater treatment plant operation by mpc based on modified asm1 with two-step nitrification/denitrification model", *Computers & Chemical Engineering*, **35**, 2469-2479, (2011).

Pereira, J., Karpinska, A., Gomes, P., Martins, A., Dias, M., Lopes, J. and Santos, R. "Activated sludge models coupled to cfd simulations", *Single and two-phase flows in chemical and biomedical engineering*, 153-173, (2012).

Rittmann, B. E. and McCarty, P. L.; "Environmental biotechnology: Principles and applications", New York, NY, *McGraw-Hill*, (2001).

Sánchez, F., Viedma, A. and Kaiser, A. "Hydraulic characterization of an activated sludge reactor with recycling system by tracer experiment and analytical models", *Water Research*, **101**, 382-392, (2016).

Tchobanoglous, G., Burton, F. L. and Stensel, H. D.; "Wastewater engineering: Treatment and reuse", New York, NY, *McGraw-Hill Professional*, (2007).

Tezel, U., Tandukar, M., Hajaya, M.G. and Pavlostathis, S.G. "Transition of municipal sludge anaerobic digestion from mesophilic to thermophilic and long-term performance evaluation", *Bioresource Technology*, **170**, 385-394, (2014).

Van Loosdrecht, M., Lopez-Vazquez, C., Meijer, S., Hooijmans, C. and Brdjanovic, D. "Twenty-five years of asm1: Past, present and future of wastewater treatment modelling", *Journal of Hydroinformatics*, **17**, 697-718, (2015).

Vanhooren, H. and Nguyen, K. "Development of a simulation protocol for evaluation of respirometry-based control strategies", *Report University of Gent and University of Ottawa*, 1996).

Vanrolleghem, P. A., Insel, G., Petersen, B., Sin, G., De Pauw, D., Nopens, I., Dovermann, H., Weijers, S. and Gernaey, K. "A comprehensive model calibration procedure for activated sludge models", *Proceedings of the Water Environment Federation*, **2003**, 210-237, (2003).

Utilization of Volcanic Tuffs as Construction Materials

Kamel Al-Zboon[1], Jehad Al-Zou'by[1] and Ziad Abu-Hamatteh[2*]

[1]*Environmental Engineering Department, Al-Huson University College, Al-Balqa Applied University, Irbid, Jordan.*
[2]*Civil Engineering Departments, Faculty of Engineering Technology, Al-Balqa Applied University, Amman (11134), Jordan*

The current study examines the possibility of utilizing the Jordanian volcanic tuff aggregates as a source of many construction materials. Different mixtures were prepared by replacing the commonly used normal aggregate with volcanic tuffs aggregate to determine the best mixing proportion with similar size in different ratios as 0, 25, 50, 75 and 100%. The impacts of this replacement on brick's compression strength, dry weight and water absorption, transverse strength, absorption and weight of terrazzo tiles, loss Anglos and CBR values have been examined and evaluated. The results revealed an improvement in compressive strength of bricks at a replacement ratio of 25%, with concomitant reduction at higher replacement ratios, while water absorption increased as the ratio of tuff increases. Transverse strength of terrazzo tiles were recorded as 6.08, 5.78, 5.78, 5.21 and 5.19 MPa at substitution ratios of 0, 25, 50, 75 and 100%, respectively. Utilization of volcanic tuffs resulted in significant reduction in the dry weight of bricks and terrazzo provided light weight material. CBR test indicated that this material can be used successfully in foundations and as a sub-base material. The obtained results buttressed the benefit of utilization natural volcanic tuffs as construction materials.

Keywords: Volcanic Tuffs; Construction Materials, Terrazzo Tiles, Bricks; Pavement Materials, Jordan.

Introduction

Selection and preparation of construction materials are of prim importance in all major engineering projects, including roads pavements, concrete mixes and other construction materials such as tiles and bricks. The engineering properties of the construction materials are supposed to meet the standards in order to achieve the minimum requirements in terms of strength and durability. (Bell, 2007). The selection of construction materials basically depends on the common index properties of rocks, such as durability, strength, density permeability and porosity. Other interference conditions such as climate conditions, project purposes and cost effectiveness should be considered during the selection and preparation process of the construction materials. The utilization of the local construction materials while maintaining the required properties and specifications represent a challenge for civil engineering all over the world (McLean and Gribble, 2005; Rahn, 1996; Johnson and DeGraff 1988). In the light of the overpoweringly increasing demand on raw materials by various construction sectors created a serious shortage in some building materials. Therefore, in order to meet the dramatic increasing demand, uncommon sources of such materials with acceptable engineering properties becomes precedence. Volcanic tuff (VT) is considered as a promising source of natural construction materials. Volcanic tuff, one of the most important natural pozzolan materials, has been used since ancient times in buildings, bridges, walls, and masonry works. Currently it is used in many countries in the world for masonry mortars, lightweight concretes and thermal for acoustic insulation materials (Balog *et al.*, 2014). Volcanic tuff with its unique structure and unique properties could serve as a construction material in many engineering projects. Tuff is a relatively soft, high porous with high surface area and low density igneous rock formed from volcanic ash or dust (Al-Zboon and Al-Zou'by, 2017). It is considered as a good inexpensive source for lightweight aggregate concrete leading to a considerable cost saving in various construction materials (Turkmenoglu and Tankut 2002; Negis, 1999; Kılınçarslan, 2011). The feasibility of using volcanic tuff as a light-weight aggregate in cement and concrete industry has been reported by many researchers (Turkmenoglu and Tankut 2002; Al-Zboon and Al-Zou'by, 2017; USBR, 1992; Kan and Gul, 1996; Kılıc et al., 2009; Augenti and Parisi, 2010; Faella et al., 1992; Smadi and Migdady, 1991; Kavasa and Evcin, 2005; Abali et al., 2006). The specific gravity of VT is about 1.84, while it is about 2.52 for ordinary sand. For this reason, VT can provide light weight concrete with density of 1440-1840kg/ m^3 in comparison with 2400kg/m^3 for normal aggregate concrete (Fredrick, 2014). Al-Zboon and Al-Zou'by (2017) used VT for concrete production and the results showed significant improvement in compressive and flexural strength at a replacement ratio of 25%, with reductions at higher ratios. Al-Zou'by and Al-Zboon (2014) utilized VT in cement mortar and found that a replacement ratio of 50% enhanced compressive strength and flexural strength. Yasin et al., (2012) studied the Jordanian tuffs for use in concrete production and they replaced 20% of the fine aggregates by volcanic tuff and thereby the concrete compressive strength improved significantly. Moreover, Fredrick (2014) replaced normal sand with VT in concrete mixes, and reported an increase in the compressive strength of concrete cubes with 2.8%, 7.4%, 11.1% and 14.0% and 5.0% for replacement ratios of 20%, 40%, 60%, 80% and 100%. In contrast, tensile strength decreased by 18.0%, 12.4%, 9.6%, 10.8% and increased (1.2%) for the same ratios respectively. Also, Smadi and Migdadi (1991) [11] used successfully VT to produce high strength lightweight concrete and achieved high compressive strength as high as 60 MPa at 90 days. Limitations of using VT in concrete mixes include but not limited to the high water absorption (11.5%), high bleeding (28ml) and low slump value (<10mm) (Al-Zboon and Al-Zou'by, 2017). Al Dwairi *et al.*, 2018 found that the replacement of normal limestone with volcanic tuff in concrete mixture resulted in increase in compressive strength, modulus of rupture, shear stress and flexural strength, while splitting strength decreased as the ratio of tuff increase.

Received on February 27, 2019; accepted on April 16, 2019 Correspondence concerning this article should be addressed to Ziad Abu-Hamatteh (E-mail address: hamatteh@bau.edu.jo). ORCID of Ziad Abu-Hamatteh: https://orcid.org/0000-0003-0929-1011

They concluded that the Jordanian tuff could be used as a lightweight concrete with good slump and absorption characteristics. Ababneh and Matalkah (2018) investigated the possible utilization of Jordanian volcanic tuff as a cementation material, and they found that JVT with high SiO_2, enhanced the compressive strength of mortars at early age (7days), while low replacement level provided better compressive strength at later age. Jordan has a huge reserve of VT mainly in the northeastern part, and the certain amount is more than two billion tons (MEMR, 2015). Nowadays, VT is used in Jordan in limited applications such as in cement production (about 400,000 ton/year), lightweight concrete and in agricultural sector. The aim of the current investigation is to evaluate the possibility of using the Jordanian VT in the production terrazzo bricks, tiles, and as pavement materials applying different ratios of VT to normal aggregates (NA). Previous studies have used limited particle size fractions of VT, whereas, the current study utilized as high as up to 100% and low down to 0% ratios of volcanic tuff as an attempted to achieve the best results. To the best of the author knowledge, this is the first time, that Jordanian tuff is used to produce bricks, terrazzo tiles and as a basement material.

2 Methodology and Materials

2.1.Materials and batching

Normal aggregate was replaced with the same size of VT at different ratios (**Table 1**), namely: B_2 (25% VT), B_3 (50%VT), B_4 (75% VT) and B5 (100%VT), in addition to the control B1 (0% VT). The properties of VT have been determined previously (Al-Zboon and Al-Zou'by, 2017), where the oven dry specific gravity ranged from 1.96 to 1.82 with absorption ratio of 10.1 and 11.5% for course and fine VT, respectively. For NA, the specific gravity ranged from 2.6 to 2.55 with absorption ratio of 1.2 to 1.7% for course and fine NA, respectively.

Table 1. Volcanic tuff and aggregate ratios in different mixture proportions.

Batch	B_1	B_2	B_3	B_4	B_5
Percent of tuff (%)	0	25	50	75	100
Percent of normal aggregate (%)	100	75	50	25	0
Weight of tuff (kg)	0	72.5	145	217.5	290
Weight of normal aggregate (kg)	290	217.5	145	172.5	0
Weight of water (kg)	18	18	18	18	18
Weight of cement (kg)	19	19	19	19	19
Total (kg)	327	327	327	327	327

Constant rate of Portland cement (200kg/m^3) was added to the aggregate component of the mix (NA and VT) and all are blended in a dry condition. Also constant amount of water (190kg/m^3) was gradually added to the mixture to achieve homogeneity and plastic form. A Mechanical mixer with volume of 0.2m^3 was used for mixing the components for the required time of 5minutes.

2.2 Molding and curing

At the end of mixing time, the mixture was poured in a container with enough size. Then, the mixture was transfer to the steel mold with internal dimension of 40x20x15cm. When the mold is full with the mixture, it is subjected to mechanical vibration and compaction hydraulic force which resulted in high density and high strength. The compacted bricks are out of the molds and put on a clean, elevated surface and labeled with the required information includes the type of batch (B_1, B_2,…) and date of production. . After drying for 24 hours, bricks were sprinkled with water for three days and then transferred to the storage for curing area according to the Jordanian standard N. 603/2 (MPWH, 1985). Twenty-four samples of bricks were taken for each mixing ratio B_1, B_2 and B_3, while only six samples were taken for B_4 and B_5, because the samples failed and did not formed as required and the material threw out after de-molding.

2.3 Laboratory tests

Upon completing the 28 days incurring period, the bricks samples were analyzed in terms of density and compressive strength according to the standard method, ASTM C67 / C67M-18. In the lab, the samples were left for one hour for drying their surface, then dimensions, and void area of bricks were determined. Initial absorption ratio was determined for three samples of each batch using oven-dried to equilibrium. Compressive strength of brick samples is determined using the hydraulic compression test machine has a maximum capacity of 2000 KN and capable to apply constant loading rate. Test procedure and speed of testing was conducted following ASTM C-67. The compressive strength of bricks was determined using the following equation:

$$F = \frac{P}{A} \quad (1)$$

Where F is the compressive strength (KN/cm^2), P is the applied force (KN), and A is the cross sectional area (cm^2) of the brick in contact with the applied force.

2.4 Utilization of Volcanic Tuff in Formulation of Terrazzo Tiles

Volcanic aggregates were added to the standard mixture with different ratios (**Table 2**). Except the tuff content, the other parameters were kept constant for all batches including: cement and water content, cement: aggregate ratio, quartz content of the top layer and mixing time. NA, VT, and cement were blended in a dry phase to achieve materials homogeneity, then water was added gradually with continuous mixing until achieving homogenous form (about 4 minutes).

Table 2. Materials used for different batches of terrazzo tiles.

Batch	T_1	T_2	T_3	T_4	T_5
Percent of tuff (%)	0	25	50	75	100
Percent of normal aggregate (%)	100	75	50	25	0
Dimension of tiles (cm)	30*30*3	30*30*3	30*30*3	30*30*3	30*30*3
Number of samples	24	24	24	24	24

2.4.1 Molding and curing

At the beginning, quartz layer with cement (10mm) was put in mechanically vibrated mold with dimension of 30x30x3cm and then the homogenous mixture was poured in the mold. After the mold is filled with mixture, it is subjected to a hydraulic force of 14N/mm^2. Then, the formed tiles were de-molded and put in humid conditions for two days. For curing purpose, samples were merged in curing tank for three days and then stored in humid conditions until the day of testing.

2.4.2 Laboratory tests

After 28 days of fabrication, terrazzo tiles samples were tested for transverse strength at drying condition, absorption and density. The specimen was placed horizontally on the bearers and subjected to loading with constant increase until the specimen fails. Transverse strength was determined for 12 samples of each batch while absorption ratio was tested for three randomly selected samples of each batch.

2.5 Utilization of Volcanic Tuff as A Pavement Material (CBR Test)

2.5.1 Material and Batching

CBR test was conducted according to D1883-07, where 5 kg sample of volcanic tuff were taken, then water was added to the sample and mixed thoroughly. Spacer disc is placed over the base plate at the bottom of the mold and a coarse filter and a paper is placed over the spacer disc. The mold was cleaned and oil was applied, then the sample was filled in the mold to the 1/5 of the total depth. The layer was compacted by giving 56 evenly distributed blows using a hammer of weight 4.89 kg. The top layer of the compacted sample is scratched and again a second layer is filled and process was repeated. After the third layer addition, the collar was also attached to the mold and process was continued. After the fifth layer collar was removed and excess materials was struck off, then the base plate was removed and the mold inverted and it was clamped to base plate. Surcharge weights of 2.5 kg were placed on top surface of sample. Three sample of coarse material (at least half the material is retained on sieve No. 200) and three samples of fine materials (materials passing sieve No. 200) were taken.

2.5.2 Laboratory test

Mold containing specimen was placed in position on the testing machine and the penetration plunger was brought in contact with the sample and a load of 4 kg (seating load) was applied so that contact between sample and plunger was established, then dial readings are adjusted to zero and load is applied such that penetration rate is 1 ±0.2 mm per minute and load was recorded. The values in N at penetrations of 2.5 and 5.0 mm were recorded and the bearing ratio for each was calculated. The greatest value calculated for penetrations at 2.5 and 5.0 mm recorded as the CBR.

$$CBR = \frac{P*100}{Ps} \quad (2)$$

Where, *P*: Measured pressure for sample (N/mm^2). *Ps*: Achieve pressure at equal penetration standard soil (N/mm^2).

2.5.3 Hardness of Raw Material

This test was conducted to determine the resistance and degradation of aggregates and its resistance to abrasion impact in the Los Angeles Machine according to ASTM C-131. The test is widely used as an indicator of the relative quality or competence of aggregates. A sample of 5 kg of coarse aggregate ware washed, and dried at the oven (103 to 105 °C) to substantially constant weight. Sample was placed in the LA abrasion testing machine, and then the machine was rotated at a speed of 30 to 33 rpm for 500 revolutions. The materials were discharged from the LA abrasion machine and separated on sieve No. 12 (1.70 mm). The weight of material coarser than sieve No. 12 was recorded, and oven-dry to a constant mass (105). After cooling, the mass was recorded.

3 Results and Discussion

3.1 Utilization of Volcanic Tuff in bricks Formulation

After 24 hours, the formed bricks were removed from the molds, and it was found that the samples number B_4 and B_5 were not formed and no cohesion occurred as the material threw out after de-molding. Samples number B_4, and B_5 with high ratio of volcanic tuff (75% and 100%), show high water absorption which decreased the available water for reaction and therefore become insufficient to complete the hydration process and subsequently to harden the bricks. Sample number B2 with 25% volcanic ratio provided the highest compression strength equal to 8.7 MPa whereas, B_1 (control) reported 6.44 MPa and finally the lowest value was recorded for B_3 with 5.96 MPa (**Figure 1.a**). Although all batches achieved Jordanian standards for unloaded bricks of 3.44 MPa (70kg/cm^2), only B_2 was comply with Jordanian standards for loaded bricks of 6.87MPa (70kg/cm^2).This result indicated that low substation of normal aggregate with volcanic tuff (25%) can be used successfully to

improve compressive strength of bricks. This result is in line with that obtained by Al-Zboon and Al-Zou'by (2017), they reported that the substitution of VT with 25% improved the compression strength of concrete.

Also, Al Dwairi *et al.*, 2018 reported that VT improved the strength characteristics of concrete. The dry weight of bricks' samples decreased from 12.8 kg/brick for B_1 to12.6 and to 11.73 kg/brick for B_2 and B_3, respectively, showing an increase in density by 2% and 8.6%, respectively (**Figure 1.b**). This reduction is probably due to the lower density of volcanic tuff in comparison with normal aggregates. In contrast, the absorption ratio increased significantly with VT increase (Figure 1 c). Higher absorption of B_2 and B_3 is attributed to the higher water absorption of the raw material (VT) due to the high voids ratio and specific surface area. Many researchers found that the adding of VT to the concrete and cement mortar mixture increased water absorption and reduced the density (Al-Zboon, and Al-Zou'by, 2014; 2017).

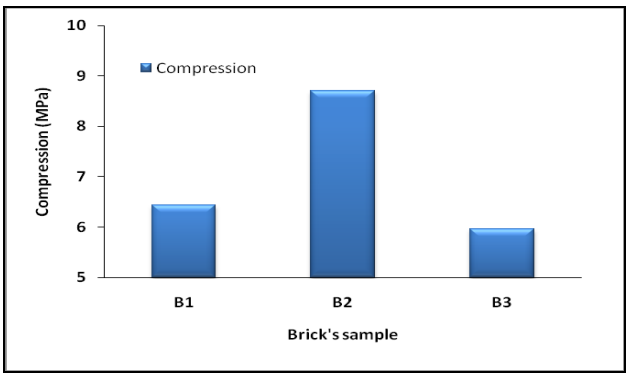

Fig. 1.a. Compression strength of bricks

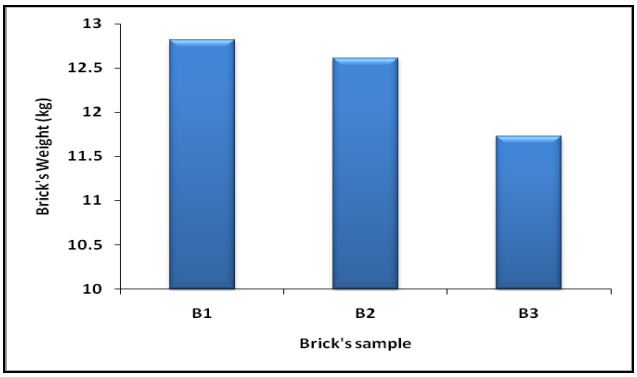

Fig. 1.b. Bricks dry weight test**.**

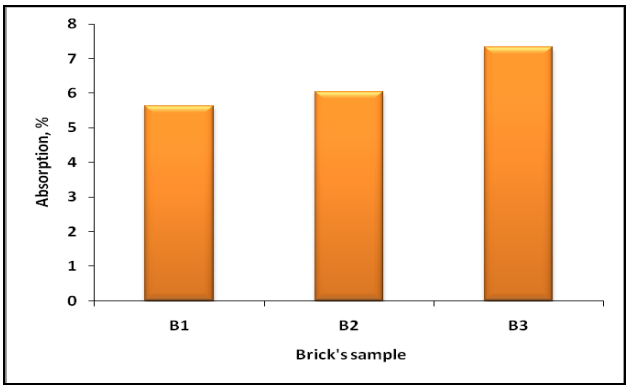

Fig. 1.c. Bricks water absorption

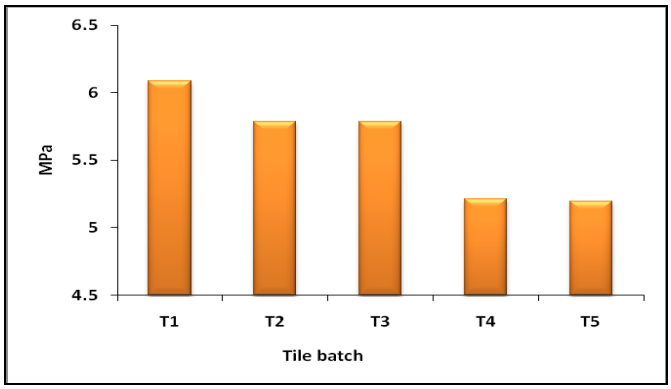

Fig. 2.a. Terazzo tiles tranverse strength

3.2 Utilization of Volcanic Tuff in Terrazzo Tiles Formulation

After 28 hours, the formed tiles were tested for transverse strength. The obtained results indicated that the average transverse strength of all tested batches exceeded the value limited in Jordanian standards (30 kg/cm^{-2}; 2.94MPa). The strength values of the tested samples ranges from 5.21-6.08 MPa in comparison with the control batch (T1), transverse strength of tiles decreased by 4.91, 4.97, 14.3, and 14.6% for T_2, T_3, T_4 and T_5, respectively (**Figure 2.a**). While T_2 and T_3 showed slight decrease in the transverse strength, T3 and T4 showed high reduction. Good strength of VT may be attributed to the high content of SiO_2 which plays significant role in the strength especially at early age of the construction material (Ababneh and Matalkah, 2018). The fine silica in VT can combine with calcium hydroxide to form stable compounds like calcium silicates, which have cementation properties (Al Dwairi *et al.*, 2018). These results revealed that the use of VT with mixture up to 50% ratio (T_3), did not affect the strength significantly. These results indicate that the volcanic aggregates could be used, with high percentage, in the bottom layer of terrazzo tiles. Regarding the density, it was found that, there is no significant difference between all samples, where the weight of a tile ranged from 7.32 for T_1, to 6.93 kg for T_5 with a 5.2% reduction (**Figure 2.b**). Lower density of produced tiles was attributed to the lower density of VT in comparison with NA as mentioned above. Kavasa and Evcin (2005) found that VT can be used successfully in the production of wall tiles with insignificant impact on the compressive strength at replacement ratio of 9, 14, 15%wt. Abu baker (2009) found that the utilization of volcanic tuff in concrete mixture resulted in a reduction in concrete density by 14%. Absorption ration increased form 1.1 for T_1 to 2.0, 2.6, 4.6, and 5.3 for T_2, T_3, T_4 and T_5, respectively (**Figure 2.c**). Due to its high voids and surface area, VT has high water absorption which explaine the obtained results. The higher water absorption at higher replacement ratio was attributed to the presence of K2O (Kavasa and Evcin, 2005).

3.3 Utilization of Volcanic Tuff as Pavement Materials (CBR Test):

Figure 3 illustrates the results of CBR test. Based on calculation, CBR for the fine and coarse materials were 28.8% and 33.33 %, respectively. Therefore, the values of CBR indicate that the materials are considered as good subsidiary for foundation and sub foundation utilization purposes (**Table 3**).

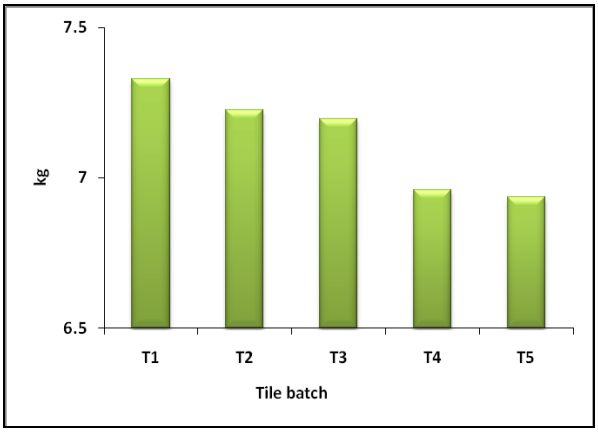

Fig . 2.b. Terazzo tiles weight

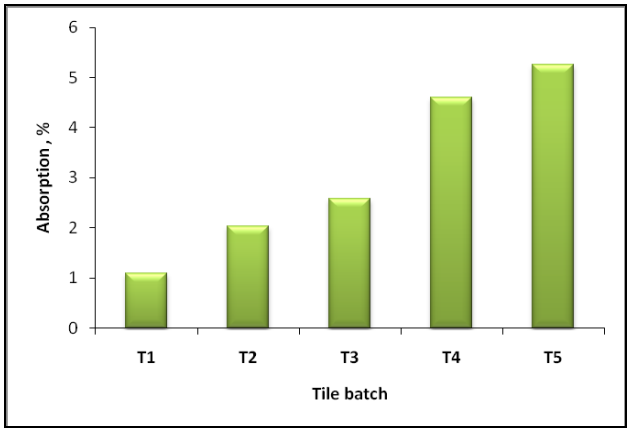

Fig. 2-c. Terazzo tiles absorption

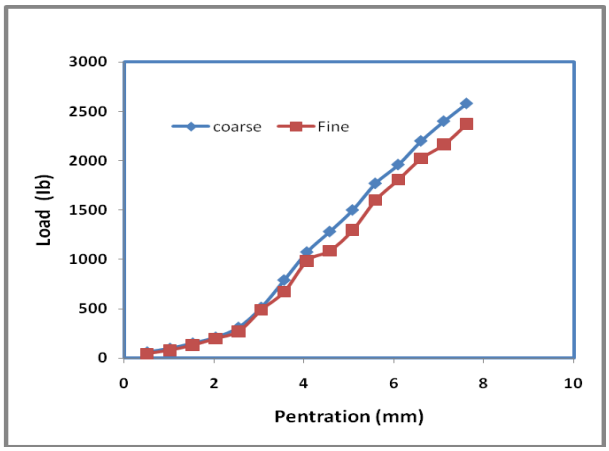

Fig. 3. Result of CBR test.

Table 3. Values of loads and its classifications for different uses.

Loading percent	Materials Classification	Field use
0-3	Very weak	Soil base
3-7	Weak	Soil base
7-2	Acceptable	Under foundation
20-50	Good	Foundation and under foundation
>50	Excellent	Foundation

The calculated Los Angeles Abrasion loss was 27.89%. There is no standard Los Angeles abrasion specification for super pavement mix design. Specifications are typically established by local agencies. Typically, U.S. specifications limit the abrasion of coarse aggregate for hot mix asphalt use to a maximum ranging from 25 to 55%, with most states using a specification of 40 or 45%. Requirements for stone matrix asphalt tend to be lower; AASHTO specifies a maximum Los Angeles abrasion loss of 30% for stone matrix asphalt. The obtained result of LA test indicated that VT complies with international standards and is suitable to be sued in hot asphalt mixes.

Conclusions

Volcanic tuff is considered an attractive and promising option to be used in various construction projects. The study indicated that bricks sample number B_2 with 25% volcanic ratio provided the highest compression strength equal to 8.7 MPa in comparison with B_1 and B_3 as the lowest value was recorded for B_3 (75%) as 5.96 MPa. Moreover, the dry weight of the sample decreased from 12.8 kg/brick for B_1 to 11.73 kg/brick for B_3, provided lower density construction material. However, the absorption ratio of samples increased from for B_1 to B_3 representing 5.63% and 7.33% respectively indicating the high water absorption of volcanic tuff. The strength values for all tested samples ranges from 5.19-6.08.0 MPa and all batches exceeded the limit of JS (2.94 MPa). These results indicate that the use of volcanic aggregate with mixture up to 50% ratio (T_3), did not affect the Terazzo tiles strength significantly. The density of tiles decreased with VT ratio increase while the absorption ratio increased accordingly. CBR test results for the fine and coarse materials were 28.8% and 33.33%, respectively. Therefore, the values of CBR indicate that the materials are considered as good pavement materials in foundation and sub foundation purposes. LA Abrasion loss was determined as 27.89% which falls within the specifications limit of coarse aggregate for hot mix asphalt. This research has the following limitations:

1. Samples of terrazzo tiles should be tested for thermal conductivity.
2. Sieve analyses should be done for the test of using VT as a pavement material.
3. It is necessary to conduct national project for utilization of VT in concrete applications.

Nomenclature

CBR: California Bearing Ratio.
MPa: Mega Pascal.

VT: Volcanic tuff.
JVT: Jordan Volcanic tuff.
NA: Normal Aggregates.
LA: Los Angeles.
P: Measured pressure for sample (N/mm^2).
Ps: Achieve pressure at equal penetration standard soil (N/mm^2).
F: Compressive strength (KN/cm^2)

References

Ababneh A., Matalkah F. "Potential use of Jordanian volcanic tuffs as supplementary cementitious materials", *Case Studies in Construction Materials*, **8**, 193-202, (2018).

Abali, Y., Bayca, S.U., Targan S, "Evaluation of blends tincal waste, volcanic tuff, bentonite and fly ash for use as a cement admixture", *Jour. Hazard Mater*., **131**, 126-130, (2006).

Abu Baker, M. Comparison of compression strength of light-weight concrete made of volcanic tuff with normal concrete. In*: 2nd International Engineering Conference*, (2009) Aden, Yemen. Available online from:http://www.adenuniv.net/uploads/conf/Engg%202/VO L%201/22.pdf.

Al Dwairi R. A., Al Saqarat, B., Shaqour,F. and Sarireh, M. "Characterization of Jordanian Volcanic Tuff and its Potential Use as Lightweight Aggregate", *Jordan Journal of Earth and Environmental Sciences*, **9**, 127-133, (2018).

Al-Zboon, K., Al-Zou'by, J. "Natural volcanic tuff for sustainable concrete industry", *Jordan Journal of Civil Engineering*, **11**, 408-423, (2017).

Al-Zboon, K., Al-Zou'by, J. "Effect of volcanic tuff on the characteristics of cement mortar". *Cerâmica*,**60,** 279-284, (2014)

Balog Anca-Andreea, Nicoleta Cobîrzan, Claudiu Aciu, Dana Adriana Iluţiu-Varvara. Valorification of volcanic tuff in constructions and materials manufacturing industry. In: T*he 7th International Conference Interdisciplinary in Engineering; Petru Maior University of Tirgu Mures*, 10-11 October 2013; Romania, 12 (2014) 323-328.

Augenti, N., Parisi, F. "Constitutive models for tuff masonry under uniaxial compression", *Jour. Mater. Civ. Eng.*, **22**, 1102-1111, (2010).

Bell, F.G. Engineering Geology, 2nd Edition, Elsevier, USA, (2007).

Faella, G., Manfredi, G., Realfonzo, R. "Cyclic behavior of tuff masonry walls under horizontal loading", In: *Proceedings of 6th Canadian Masonry Symposium*; Canada, 317-328, (1992).

Fredrick, O. S. "A study into the performance of volcanic tuff as partial replacement of river sand in pre-cast concrete", F16/29021/2009 5th year project report (2014).

Johnson R. B, and De Graff, J. V. Principles of Engineering Geology, Wiley, (1988).

Kan, A., Gul, R. "Properties of volcanic tuff sands as a new material for masonry mortar", *International Journal of Natural and Engineering Sciences* **2**, 69-74, (1996).

Kavasa, T., Evcin, A "Use of Afyon region (Turkey) volcanic tuffs in wall tile production", *Industrial Ceramics*, **25**, 17-19,. (2005).

Kılıc, A., Ati, C. D. Teymen, A. Karahan, O. Kamuran, A. "The effects of scoria and pumice aggregates on the strength and unit weight of lightweight concrete", *Sci. Res. Essays*, **4**, 961-965. (2009).

Kılınçarslan, S. "The effect of zeolite amount on the physical and mechanical properties of concrete", *Int. J. Phys. Sci.*, **13**, 3041-3046, (2011).

McLean, A.C. and Gribble, C.D. Geology for Civil Engineers, 2nd Ed., University of Glasgow, Taylor & Francis, (2005).

MEMR , Ministry of Energy and Mineral Resources: Mineral Status and Future Opportunity, Volcanic tuff; (2015). Available online from: http://www.memr.gov.jo/EchoBusV3.0/SystemAssets/PDFs/AR/MineralTR/Zeolitic%20Tuff.pdf.

MPWH , Ministry of Public Works and Housing. Specifications of the architectural and civil works, 1st Edn.. Amman, Jordan (1985).

Negis, F. Zeolite-based composites in energy storage, master dissertation, Izmir, Turkey: Izmir Institute of Technology. (1999).

Rahn P.H. Engineering Geology: An Environmental Approach, 2nd Ed., Prentice Hall, (1996).

Smadi, M. M., Migdady, E. "Properties of highstrength tuff light-weight aggregate concrete", *Cement Concrete Comp.*, **12**, 129-135, (1991).

Turkmenoglu, A.G., Tankut, A. "Use of tuffs from central Turkey as admixture in pozzolanic cement assessment of their petro-graphical properties", *Cement Concrete Res.*, **32**, 629-637, (2002).

U.S. Bureau of Reclamation (USBR). Concrete Manual, Part 2: A Manual for the Control of Concrete Construction, 9th Ed. Water Resources Technical Publication, U.S. Department of the Interior, Technical Services Center, USBR, Denver, Colorado. (1992).

Yasin, A., Mohammed, T. A., Hassan, R. H., Eid, I.S. "Effect of volcanic tuff on concrete compressive strength", *Contemp. Eng. Sci*,. **5**, 295-306, (2012).

AL-BALQA APPLIED UNIVERSITY

Hashemite Kingdom of Jordan

Scientific Research Support Fund

المجلة الأردنية للهندسة والصناعات الكيميائية

April 2019 | VOLUME 02 | NUMBER 01

ISSN 2616 - 9584 (Online)
ISSN 2616 - 9584 (Print)

JJECI

www.jjeci.com

info@jjeci.com

مجلة علمية عالمية متخصصة محكمة

تصدر بدعم من صندوق دعم البحث العلمي